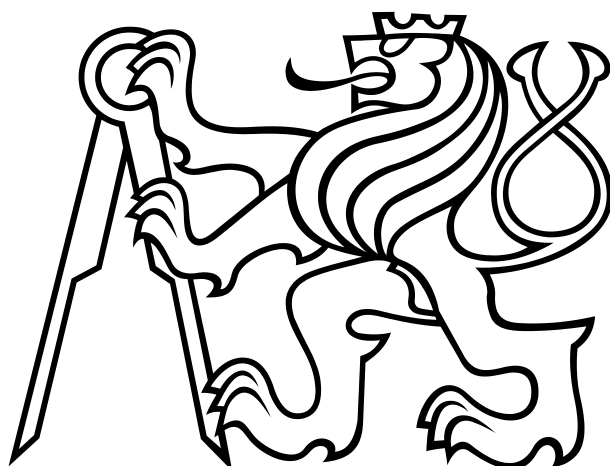CZECH TECHNICAL UNIVERSITY IN PRAGUE
FACULTY OF ELECTRICAL ENGINEERING
Cybernetics and Robotics

BACHELOR THESIS

CHARGED PARTICLE MOTION IN ION ENGINE NEAR THE VALIDITY OF ADIABATIC APPROXIMATION

Author
Matúš Cvengroš

Supervisor
prof. RNDr. Petr Kulhánek, CSc.

May 2013

České vysoké učení technické v Praze
Fakulta elektrotechnická

katedra řídicí techniky

ZADÁNÍ BAKALÁŘSKÉ PRÁCE

Student: **Matúš Cvengroš**

Studijní program: Kybernetika a robotika
Obor: Systémy a řízení

Název tématu: **Pohyb nabitých částic v iontovém motoru na hranici platnosti adiabatického přiblížení**

Pokyny pro vypracování:

1. Nastudujte teorii adiabatického přiblížení a z ní plynoucí driftovou rovnici a teorii driftů.
2. Sestavte numerický model pro pohyb částice v obecném magnetickém poli kombinovaném s dalším polem.
3. Řešte pohyb nabitých částic minimálně ve dvou konfiguracích.
4. Porovnejte numerické řešení s adiabatickým přiblížením.
5. Stanovte pro obě situace podmínky, za kterých je adiabatické přiblížení ještě fyzikálně akceptovatelné.

Seznam odborné literatury:

[1] Kulhánek P: Úvod do teorie plazmatu; AGA 2011
[2] ESA portal: Ion engine systems
[3] Shabana A: Computational Dynamics; Willey 2010

Vedoucí: Prof.RNDr. Petr Kulhánek, CSc.

Platnost zadání: do konce zimního semestru 2013/2014

prof. Ing. Michael Šebek, DrSc.
vedoucí katedry

L.S.

prof. Ing. Pavel Ripka, CSc.
děkan

V Praze dne 13. 11. 2012

PREHLÁSENIE

Prehlasujem, že som predloženú prácu vypracoval samostatne a že som uviedol všetky použité informačné zdroje v súlade s Metodickým pokynom o doržiavaní etických princípov pri príprave vysokoškolských záverečných prácach.

V Prahe, dňa ___24. 5. 2013___

_____
podpis

iv

ACKNOWLEDGEMENT

ABSTRAKT

Hlavným cieľom tejto práce bolo štúdium pohybu nabitých častíc vo výbojovej komore Hallovho iontového motoru pri pôsobení axiálneho elektrického a radiálneho magnetického poľa. V priebehu celej práce sa využíva adiabatické priblíženie, ktoré je hlavne na konci spomenuté a následne detailnejšie rozpracované. V teórii sa zoznamujeme so základnými princípmi elektromagnetizmu, ktoré sú následne aplikované na konkrétnejšie odvodenie fyzikálnych vlastností Hallovho motoru. Kvôli problematike pohybu nabitých častíc bola vysvetlená aj Lorentzova pohybová rovnica, odvodená taktiež pre relativistické prípady, ktorá je v tomto prípade základnym aspektom tvorby diferenciálnych pohybových rovníc. Taktiež bolo navrhnuté elektrické a magnetické pole, ktoré reprezentuje aproximáciu polí nachádzajúcich sa v Hallovom iontovom motore. Následne je v práci spomenutý aj úvod do numerických metód výpočtu riešení diferenciálnych rovníc, ktoré sú obratom aplikované na vytvorenie simulácií pohybu častíc v Hallovom motore.

ABSTRACT

Main goal of this thesis is the study of charged particle motion in discharge chamber of Hall ion thruster with impact from axial electric and radial magnetic field. Throughout the work we use the theory of adiabatic approximation, which is mentioned mainly at the end and subsequently described in more details. In theory, we are discussing basic principles of electromagnetism, which are applied on more specific derivation of physical attributes of Hall effect ion thruster. Because of actual charged particle motion, Lorentz equation was explained and derived for relativistic case, as in our case it is the main aspect of creating differential equations of motion. Also, electric and magnetic field was designed, representing approximation of real fields that take presence in Hall ion thruster. Later on we move to introduction to numerical methods for computing solutions of equations of motion, where these methods are applied for simulations of charged particle motion inside of Hall effect ion thruster.

CONTENTS

LIST OF FIGURES

NOMENCLATURE

α	Relativistic constant	[–]
Δv	Change of spacecraft's velocity between two time-stamps	[m/s]
$\dot{m}$	Change of spacecraft's mass due to propellant consumption	[kg/s]
$\dot{m}_{\text{ions}}$	Ion beam mass flow	[kg/s]
$\dot{m}_{\text{ppl}}$	Change of propellant mass over time	[kg/s]
ϵ_0	Electric permittivity of vacuum	[F/m]
γ	Relativistic constant	[–]
$\mathcal{N}_{\text{i}}$	Ion flow	[ions/s]
$\mathcal{T}_{\text{e}}$	Kinetic energy of electron	[J]
$\mathcal{T}_{\text{ions}}$	Kinetic energy of ion beam	[J]
$\mathcal{T}_{\text{p}}$	Kinetic energy of particle	[J]
$\mathcal{U}$	Energy of electron produced by electrode	[J]
$\mathcal{V}_{\text{p}}$	Potential energy of particle	[J]
μ_0	Permeability of vacuum	[H/m]
$\phi(\mathbf{r})$	Potential of electric field in position $\mathbf{r}$	[V]
ϕ_{A}	Potential of anode	[V]
ϕ_{C}	Potential of cathode	[V]
θ_{EB}	Angle between electric and magnetic field in a given point	[rad]
$\hat{\mathbf{B}}$	Unit vector of magnetic inductance	[–]
$\hat{\mathbf{E}}$	Unit vector of electric intensity	[–]
$\hat{\mathbf{r}}_{\text{z}}$	Unit vector in the z direction	[–]
$\boldsymbol{\nabla} B$	Gradient vector of magnetic induction	[T/m]
$\mathbf{B}$	Vector of induction of magnetic field	[T]

$\mathbf{E}$	Vector of intensity of electric field	[V/m]
$\mathbf{E}_\mathrm{A}$	Vector of electric field produced by anode	[V/m]
$\mathbf{F}_\mathrm{C}$	Coulomb force vector	[N]
$\mathbf{F}_\mathrm{e}$	Force vector acting on electron	[N]
$\mathbf{F}_\mathrm{i}$	Force vector acting on a single ion	[N]
$\mathbf{j}_\mathrm{Hall}$	Hall current density	$[\mathrm{C} \times \mathrm{m}^{-2} \cdot \mathrm{s}^{-1}]$
$\mathbf{p}_\mathrm{e}$	Momentum of electron	$[\mathrm{kg} \cdot \mathrm{m/s}]$
$\mathbf{p}_{\mathrm{M_c}}$	Magnetic moment of core magnet	$[\mathrm{A} \cdot \mathrm{m}^2]$
$\mathbf{p}_{\mathrm{M_j}}$	Magnetic moment of slave magnet	$[\mathrm{A} \cdot \mathrm{m}^2]$
$\mathbf{p}_\mathrm{M}$	Vector of magnetic dipole moment	$[\mathrm{A} \cdot \mathrm{m}^2]$
$\mathbf{r}$	Position vector to a random given particle	[m]
$\mathbf{r}'$	Position vector to a random supplementary particle	[m]
$\mathbf{r}_{\mathrm{B_0}}$	Position of nominal value of magnetic field	[m]
$\mathbf{r}_\mathrm{c}$	Vector of core magnet offset coordinates	[m]
$\mathbf{r}_{\mathrm{e_{init}}}$	Initial position of electron	[m]
$\mathbf{r}_\mathrm{elctr}$	Position of electrode	[m]
$\mathbf{r}_{\mathrm{i_{init}}}$	Initial position of ion	[m]
$\mathbf{r}_\mathrm{j}$	Vector of supportive magnet offset coordinates	[m]
$\mathbf{T}_\mathrm{i}$	Thrust force vector produced by single ion	[N]
$\mathbf{v}_{\mathrm{e_0}}$	Initial velocity of electron	[m/s]
$\mathbf{v}_\mathrm{e}$	Velocity vector of electron	[m/s]
$\mathbf{v}_\mathrm{i}$	Velocity vector of accelerated ion	[m/s]
$\mathbf{v}_{\mathrm{p r_0}}$	Velocity vector of particle in position $\mathbf{r}_0$	[m/s]
$\mathbf{v}_{\mathrm{p r}}$	Velocity vector of particle in position $\mathbf{r}$	[m/s]
c	Speed of light	[m/s]
d_AC	Distance between anode and cathode	[m]
d_C	Distance from cathode	[m]
g	Gravitational acceleration	$[\mathrm{m/s}^2]$

I	Current generated by an elementary charge	[A]
I_{sp}	Specific impulse	[s]
m	Mass of entire spacecraft	[kg]
$m_{\mathrm{e_0}}$	Rest mass of electron	[kg]
m_{e}	Mass of electron	[kg]
$m_{\mathrm{i_0}}$	Rest mass of ion	[kg]
m_{ions}	Mass of all ions combined	[kg]
m_{i}	Mass of single ion	[kg]
m_{ppl}	Propellant mass	[kg]
m_{p}	Mass of particle	[kg]
N_{A}	Avogadro constant	[particles/mol]
n_{e}	Electron density	[electrons/m^3]
N_{i}	Number of ions	[ions]
n_{i}	Ion density	[ions/m^3]
P_{ions}	Power of ion beam	[W]
Q	Elementary charge	[C]
q	Charge of source particle or point charge	[C]
Q_{p}	Charge of particle	[C]
R_{A}	Major radius of anode	[m]
r_{A}	Minor radius of anode	[m]
S'	Supplementary surface	[m^2]
S_{A}	Surface area of anode	[m^2]
T	Thrust produced by the engine	[N]
t_{final}	Final time	[s]
t_{init}	Initial time	[s]
U	Potential difference	[V]
v_{ex}	Exhaust velocity	[m/s]
v_{ions}	Leaving velocity of ions	[m/s]

$v_\perp$	Drift velocity perpendicular to both electric and magnetic fields	[m/s]
W_ions	Total work of all ions moving between two separate potentials	[J]
W_p	Work done by field to move particle	[J]
$W_\text{p}(C)$	Work done by field to move particle following trajectory C	[J]
y_0	Position of nominal magnetic field on y axis	[m]

CHAPTER 1
GENERAL OVERVIEW OF ION THRUSTERS

1.1 HISTORY AND ORIGINS

It is said that the father of the concept of electric propulsion engine is **Konstantin Tsiolkovsky**, as he is the first person to publish the idea in 1911. First document was however written by **Robert H. Goddard**, an American rocket pioneer, who experimentally tested the concept at Clark University in years $1916 - 1917$.

1.2 OVERVIEW OF ELECTRIC PROPULSION ENGINES

Various forms of electric propulsion engines exist, however there are few that are being used for decades and few that are purely experimental. Ion thrusters are at the highest level categorized into two possible options, which are:

- Electrostatic Ion Thruster
- Electromagnetic Ion Thruster
- Electrothermal Ion Thruster

Their name is derived from the type of force they are using to accelerate the ions of ionized gas. While electromagnetic thrusters use **Coulomb force** in order to provide acceleration, electromagnetic thrusters use **Lorentz force**. Coulomb and Lorentz force will be discussed later.

Three main categories exists which work on **electrostatic principle**. They are:

- Gridded Electrostatic Ion Thruster
- Hall Effect Ion Thruster
- Field Emission Electric Propulsion (FEEP)

Electromagnetic thrusters are divided into two main categories:

- Pulsed Plasma Thruster (PTT)
- Magnetoplasmadynamic Thruster (MPD)

and **electrothermal thrusters** are:

- Resistojet
- Acrjet
- Variable Specific Impulse Magnetoplasma Rocket (VASIMR)

We will discuss and briefly describe the function of some of the mentioned thrusters, focusing mainly on **Hall effect ion thruster**, as this is the main topic of this thesis.

1.3   GRIDDED ELECTROSTATIC ION THRUSTER

This type of thruster was the first to be introduced into commercial space flights and it is mainly used as a propulsion for geostationary orbit keeping.

As a propellant, xenon gas is used, which is inert and with neutral charge in its normal form. Molecules of xenon are bombarded with electrons with enough kinetic energy to detach more electrons which are then extracted, thus leaving a positively charged ions. These ions are simply accelerated through two (in the most simplest form) or through series of electrically charged grids. A reader can simply imagine that ions are accelerated between two charged plates of any material that provides ability to store enough charge, however those plates are filled with holes. That way, ions are actually able to escape.

After acceleration, another external cathode emits extracted electrons into the ion beam, making it neutrally charged as it escapes the vehicle. That way, not only they do not return to vehicle (which will cancel the thrust produced), but also prevent from building negative charge on vehicle, which could have fatal consequences on electronics on board. Diagram showing the working principle of such an engine is in the figure 1.1.
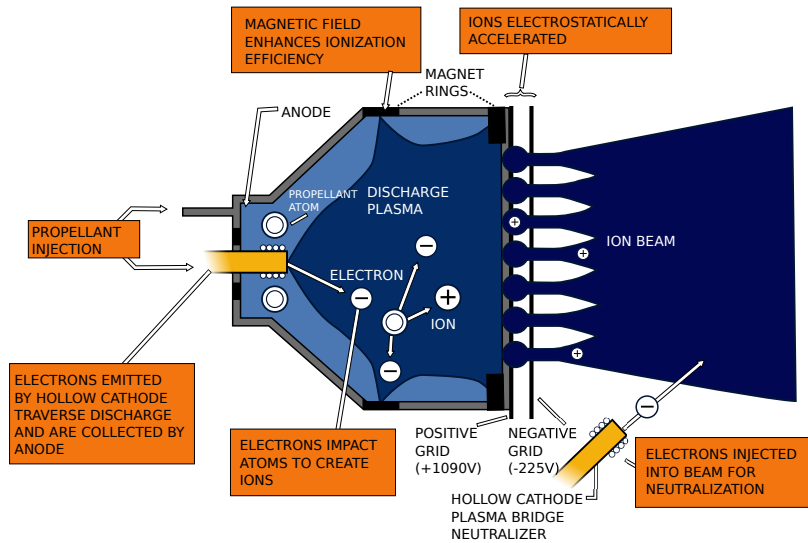
Figure 1.1: Deep Space 1 Ion Engine working principle. Image: NASA Glenn Research Center.

In this design, ions accelerated towards the negatively charged accelerator grid can cause erosion. End-of-life is reached when either a structural failure of the grid occurs or the holes in the accelerator grid become too large. This erosion cannot be avoided and is the major life–limiting factor of gridded ion thruster.

Russia has successfully used ion engines during years 1950–1960, however first major success of this technology was in late-1990s, where electric thruster was first time used on interplanetary probe **Deep Space 1**. Main mission of this probe was to reach and photograph small planet **9969 Braille**, where ion engine **NASA Solar electric propulsion Technology Application Readiness (NSTAR)** was used as the one and only propulsion system to achieve this goal. More about the engine can be found in [7]. More

about the probe in [5] or [1].

Since gridded ion thrusters are not the main purpuse of this thesis, we will move further, however one can read more about this particular topic, for instance, in [4].

1.4   HALL EFFECT ION THRUSTER

Hall effect thrusters use electric potential difference for particle acceleration the same way as gridded ion thrusters. That is the reason they are sometimes referred to as gridless ion thrusters. Even that this naming is far from the proper description of how do they work, it is providing a good starting point of describing their operation.

1.4.1   HISTORY OVERVIEW

First Hall effect thrusters were designed in United States in 1960s, however they were abandoned, since US scientists at NASA focused more on the development of gridded ion thrusters. In Soviet Union however, research continued around year 1970, where two basic types of thrusters were developed: the Stationary Plasma Thruster (SPT), developed under the leadership of A. I. Mozorov at the Kurchatov Institute, and the Thruster with Anode Layer (TAL), developed under leadership of A. V. Zharinov at TSNIIMASH [6]. These two types of thrusters will be discussed later. Russia has been using these thrusters since those years in many space probes, where malfunction was never observed. One could say that Russians always knew what to do when it comes to deal with space. After this success, US was again interested in Hall thrusters, where research continued also in NASA, mainly Jet Propulsion Laboratory and Glenn Research Center, around 1990s.

In 2003, European Space Agency used Hall thruster in space probe named SMART-1 (*Small Missions for Advanced Research in Technology*), for interplanetary travel. In 3 years, continuous function of the Hall thruster present allowed probe (with gravitational help of Earth) to achieve Moon operational orbit by a spiral trajectory. Mission objective was primarily to test the ion engine, which was highly successful. Probe crashed on moon surface on purpose, on 3rd of September 2006 at speed around 2000 km/s. More on this topic in [2].

1.4.2   THRUSTER DESIGN AND PRINCIPLES

Hall effect ion thruster consists of three main parts. First is electric circuit consisting of annular anode and a cathode, where anode also serves as gas distribution device, as it is filled with small holes, which gas can easily pass through. Space where ions are accelerated, known as **discharge chamber**, is the second main part of the engine, created from a ceramic material to prevent erosion and heat generated by plasma. Third one is magnetic field produced by inner core electromagnet and outer slave electromagnets.

Electrons are emitted from cathode, which are then trapped in radial magnetic field created by electromagnets. This magnetic field is known as **magnetic dipole**, and is created, for instance, by a closed loop of current flowing through a coil. These electrons

experience gyrating motion around the inner electromagnet (from now on *core* electromagnet), and are freed only by collisions with accelerated ions or by collisions with the walls of the discharge chamber, thus completing the electric circuit. Electron motion around this core is caused by the force that is acting on these electrons, which is result of the $\mathbf{E} \times \mathbf{B}$ cross field, where $\mathbf{E}$ is axial electric field created by anode. This motion is known as *Hall current* and is the reason why device got its name. Reader skilled in electromagnetism may now think that the azimuthal drift is caused also by an additional electron drift, which is caused by forces such as centripetal force. This electron motion would be interpreted as *closed–drift* and could remind of motion particles experience in magnetrons, however this is not true, since the reason for azimuthal drift is force related only to cross product of electric and magnetic field. This force is largest in those points where the direction of velocity vector $\mathbf{v}_e$ is parallel to vector of magnetic field $\mathbf{B}$, as shown in figure 1.3. Reason why this drift is not a closed–drift is simply because of the secondary electromagnets, which are in combination with core creating magnetic field that is enclosed after the boundary of discharge chamber. Following figures 1.2a and 1.2b shows the difference between both cases.

(a) Boundary of discharge chamber located after magnetic field is closed.

(b) Boundary of discharge chamber located before magnetic field is closed.
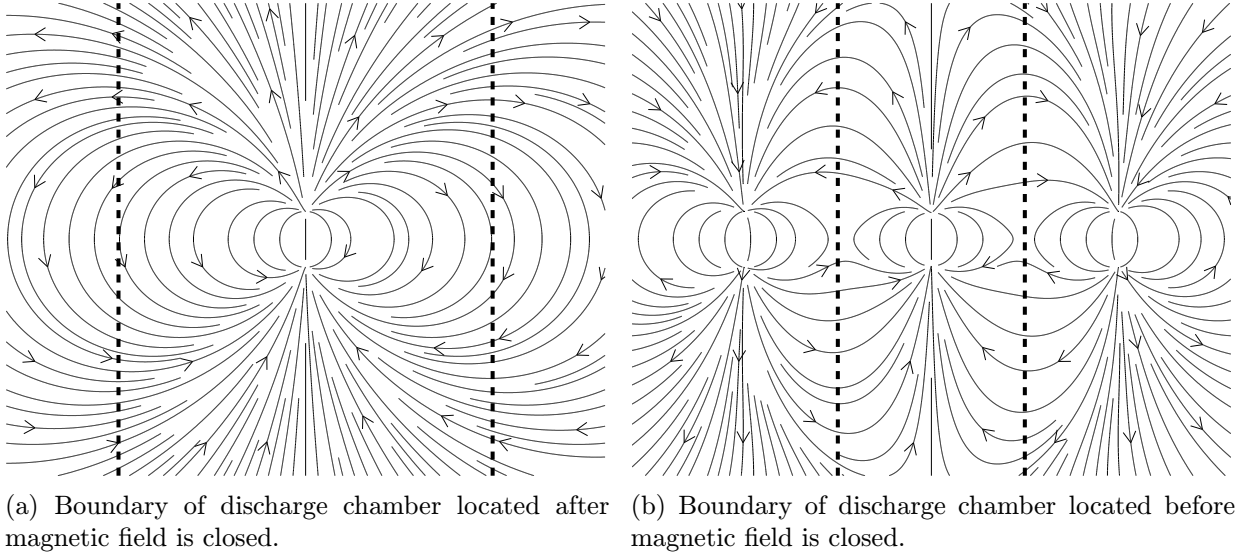
Figure 1.2: Various enclosure of magnetic fields.

Moving electrons are also responsible for ionization of xenon gas through collisions, where after these collisions (or collisions with the boundary of discharge chamber) they close the circuit by flowing into anode. When gas is ionized, ions of xenon feel the potential difference not only by positively charged anode, but also by negatively charged rotating circle of electrons, something as a *virtual cathode*. It is due to this behavior that engine is also known as gridless ion engine. Important thing is to design magnetic field in such a way that electrons are trapped, but much more heavier ions of xenon are able to escape into space.

As was said earlier, two main types exists, which are SPT and TAL Hall thrusters. Discharge chamber of SPT is made purely of ceramic material, mostly in annular form. In TAL, anode is composed of a cone–shaped form, where walls of discharge chamber are
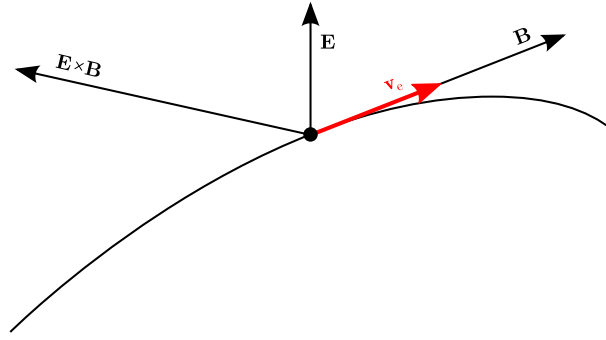
Figure 1.3: Moving electron is experiencing largest force when is moving parallel to lines of magnetic field.

enclosed in *guard rings*, which are commonly charged at the cathode potential, to repel moving electrons and thus prevent electron losses. Basic principle of work, however, stays the same for both of them. Difference in geometry between SPT and TAL are illustrated in figures 1.4a and 1.4b.

(a) Geometry of SPT Hall Thruster.

(b) Geometry of TAL Hall Thruster.
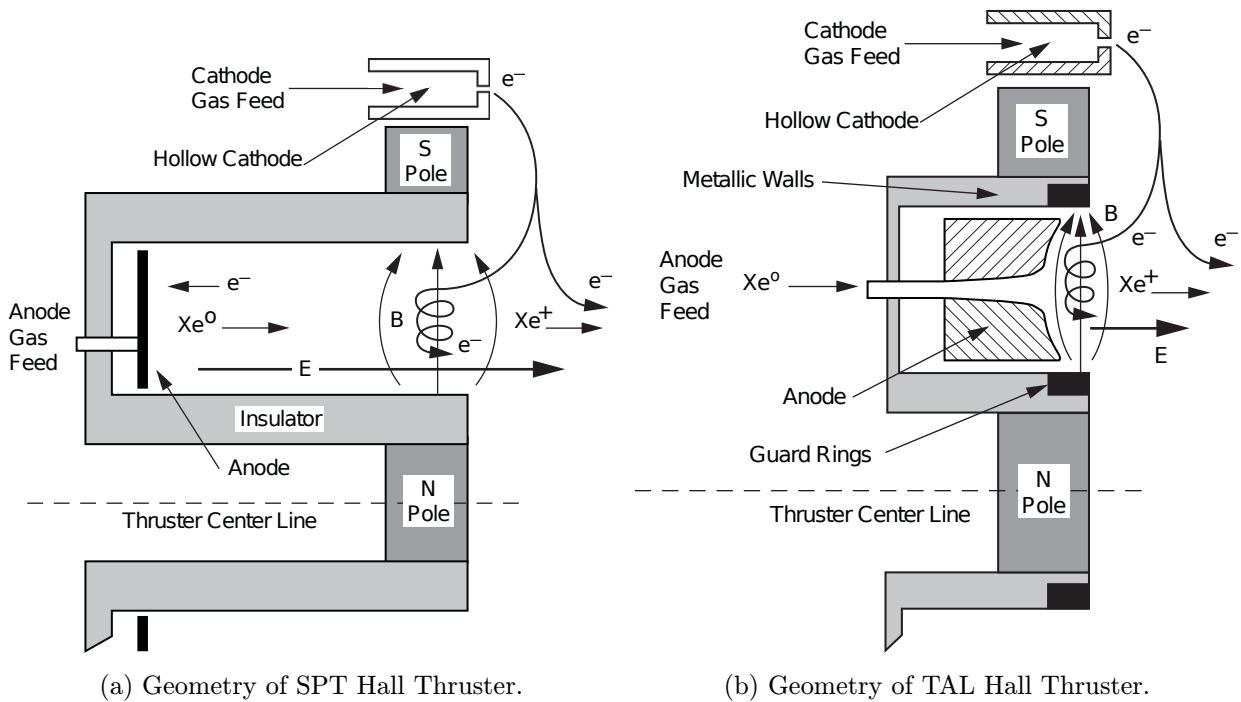
Figure 1.4: Differences in geometries between SPT and TAL Hall Thrusters. Images: Fundamentals of Electric Propulsion: Ion and Hall Thrusters [4]

Designing a Hall thruster is even in these days still more of an empirical science, where one must rely on experience of what was done in the past, mostly by Russians in 1960s. Hall thrusters are mostly configured in 5 electromagnet configuration, where core magnet is in the center and 4 support magnets are located around the core by 90° azimuthally, however if more support magnets are present, magnetic field created is more balanced and stable. Possible configuration is shown in figure 1.5. Hall ion thrusters are often in scale of centimeters, maximum tenth of centimeters, but smaller thrusters are also possible. For instance, in early stages of research made in Soviet Union, many SPT and TAL thrusters

were designed with markings such as *SPT-100* or *D-55 TAL*, where number suffix means diameter of the discharge chamber in millimeters.
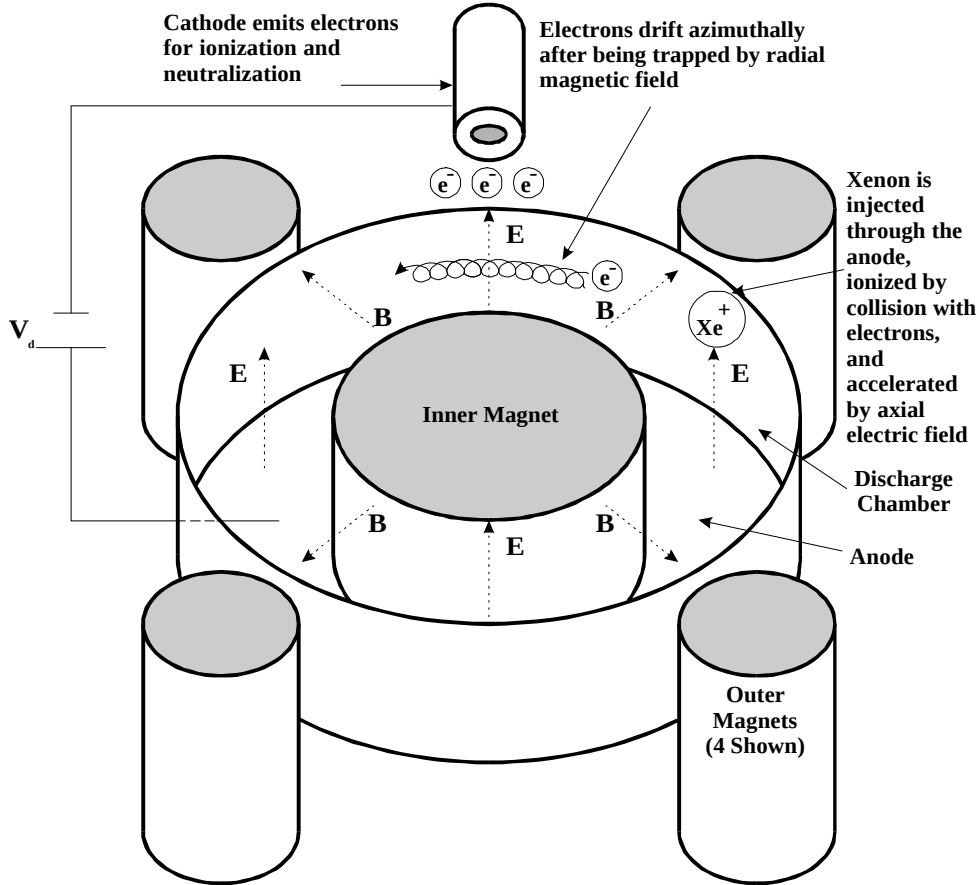
Figure 1.5: Possible configuration of Hall Ion Thruster. Image: Figure from Ph.D. Thesis of Frank Stanley Gulczinski III [6].

For designing a Hall ion thruster, one must know few important equations. They were done as trial-error method by Russian scientists, and although we currently have means for numerical methods, it is always good to know rough numbers needed for first design characteristics. However, purpose of this thesis is not to design a Hall thruster ion engine not even in a closest approximation, but rather study particle motion in electromagnetic field which is present in such a thruster. If reader would want to study these parameters, they can be found in [6], although they may be outdated and not accurate, due to the year of publication of this work. This is another reason why they are not presented in this thesis.

Anode and discharge chamber does not have to be always annular, but it is preferred in thrusters with rather greater dimensions, since annular discharge chamber has proven as the one with the best efficiency possible. This rule does not apply when scaling into small proportions, where rather cylindrical shaped thrusters are designed. Example of Hall thruster hot firing is in the figure 1.6.

Figure 1.6: Hot firing of Hall Ion Thruster. Image: Alta–Space.

1.5 MAGNETOPLASMADYNAMIC ION THRUSTER

This particular ion engine will be discussed in a slightly wider form than gridded electrostatic ion engine, but less than Hall effect thruster. Reason of this is because of its promising potential for my study in upcoming years, since I would like to continue in my research focusing primary on this type of engine, where this current bachelor thesis is a preparation for my research and work that would have to be done in future.

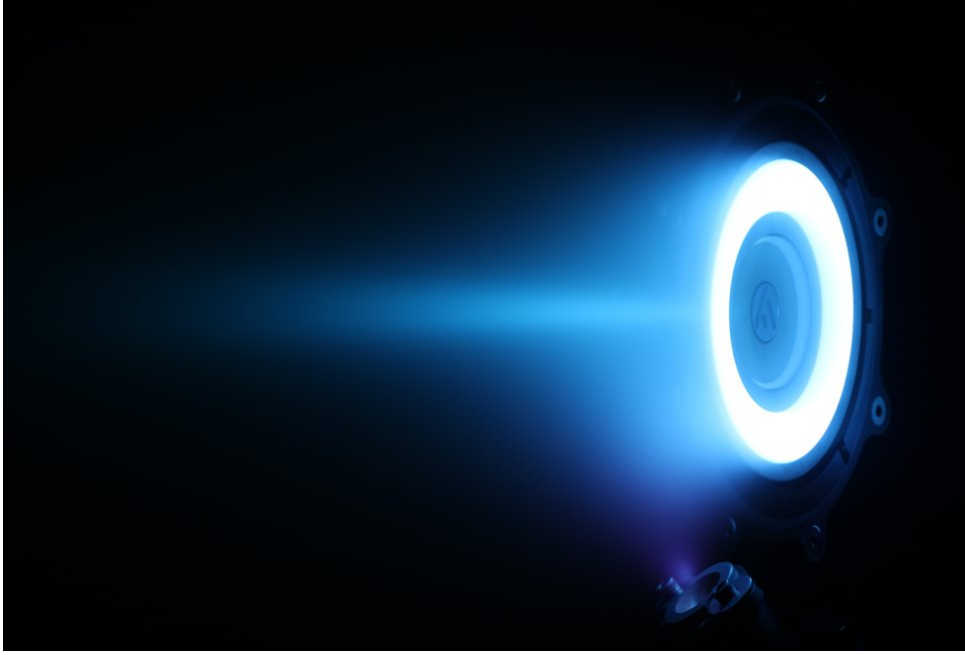Magnetoplasmadynamic ion thruster (MPD) belongs to the class engines which uses *Lorentz Force* for acceleration of particles. Directly Lorentz Force will be discussed in section 2. Where electrostatic ion thrusters used magnetic field only for some parts of the engine or omitted magnetic field entirely, in MPD thruster, magnetic field is essential not only for its overall function, but primary for acceleration.

Engine consists of so called acceleration chamber, where (mostly) *xenon* gas is also ionized. Following parts are anode and cathode. Principle of engine operation is surprisingly the easiest of all previously described, however the most complicated one for simulations with impossible or very limited analytical possibilities of description of electromagnetic fields that are occurring inside the engine. Gas is injected through a protective layer at the rear end of thruster, where it is subsequently prepared for ionization. High electric potential is brought to anode, which is in closed distance with cathode. This arrangement of electrodes creates closed current arc, that ionizes gas, thus creating plasma. Moving electrons which produce current also produce *self–induced* magnetic field, as shown in figure 1.7. This field is perpendicular to the motion of electron, thus perpendicular to electric field. When ions feel this cross fields, they immediately start moving out of the engine, following the law of Lorentz Force.
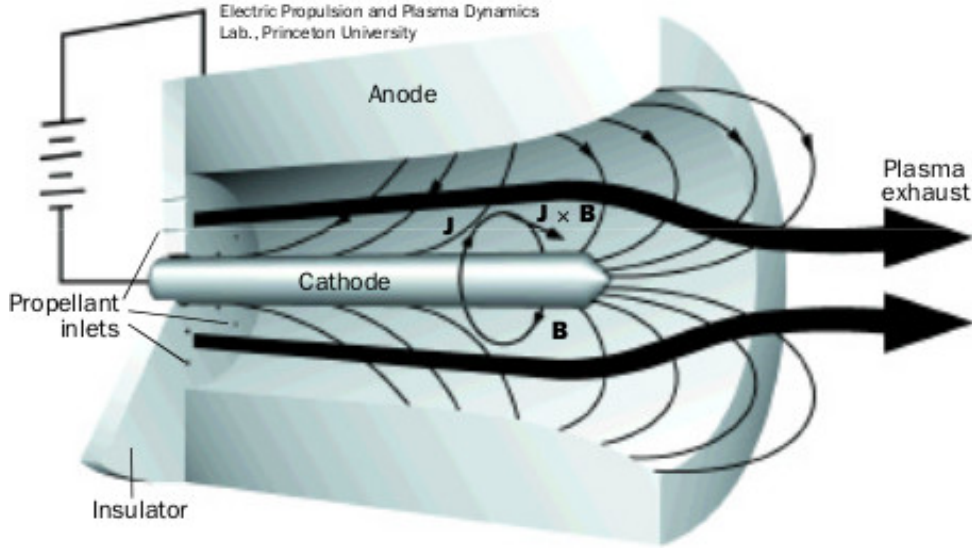
Figure 1.7: MPD Thruster principles. Image: Electric Propulsion and Plasma Dynamics Lab., Princeton University.

These thrusters are divided into two major categories based on the method of generating magnetic field. We already named the first one in previous paragraph, which are MPD thrusters with self–induced magnetic field. Second group are MPD thrusters with applied magnetic field. We will not go into the details of plasma motion, however the main reason for application of external magnetic field is because of plasma stabilization. Differences in both self–induced and applied MPD thrusters is shown in figures 1.8a and 1.8b.

(b) MPD Thruster with applied magnetic field.

(a) MPD Thruster with self–induced magnetic field.
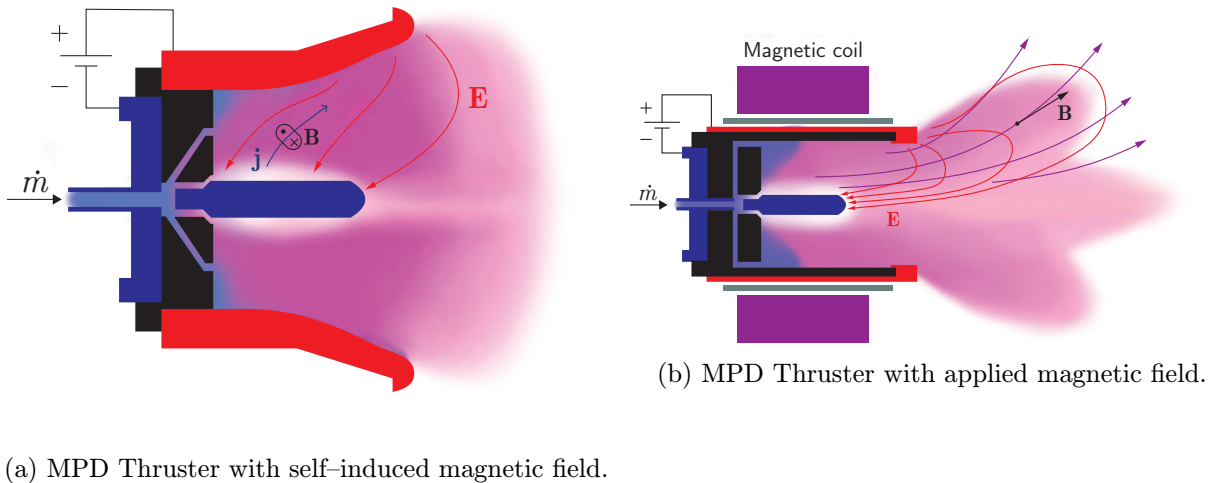
Figure 1.8: MPD Thruster types.

MPD thrusters have advantage of very high thrust they can produce, holding all of the capabilities of ion thrusters. However, everything has a price, and MPD thrusters are not any different. In contrast with Hall effect or gridded ion thrusters working in range of W to kW, MPD thrusters work in range of hundreds of kW or even MW. Such energetic

abilities do not cover any of today technologies for creating electricity in space and that is the reason why MPD thrusters are discussed only theoretically. If physically designed, then only for purposes of ground testing. However, they are the best candidate for interplanetary travel, and that is the reason why MPD thrusters were mentioned in this document and will also have my focus in future research.

1.6 VARIABLE SPACIFIC IMPULSE MAGNETOPLASMA ROCKET

Though this type of thruster is highly theoretical (with only few corporations currently developing it), we will mention it because of the unique capabilities it preserve.

VASIMR is electrothermal thruster, which means that the propellant is heated to high temperatures and then expanded. Heating is generated in two phases. In the first one, *Helicon Antenna* heats up gas to temperature up to 5000° and thus creating *cold plasma*. Second is *ICRH Antenna*, where plasma is heated up to millions of degrees Kelvin. Both stages are shown in figure 1.9.
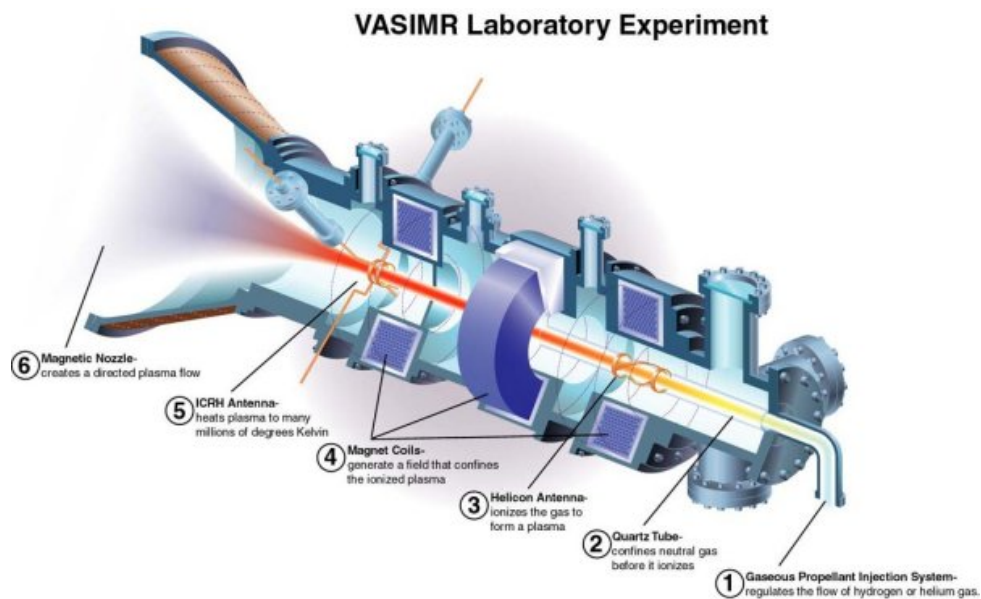
Figure 1.9: VASIMR thruster principles.

Magnetic field applied is parallel to axial axis of the engine, making ions to orbit around the inner part of heating chamber. Since ions are orbiting around axial axis and high temperatures create pressure, ions are moving towards the end of engine, producing electric field. Another radial magnetic field located around the nozzle creates cross field with electric field and redirects ions out into the space.

VASIMR engine has two key advantages: electrodeless design and capability to create variable specific impulse due to variable heating and magnitude of radial magnetic field, which gave the system its name.

CHAPTER 2
HALL THRUSTER PHYSICS

In following sections, we will discuss and introduce basic laws and principles that allow us to theoretically formulate Hall thruster properties. It is important to note that most of the calculations will be made non–relativistic, since exhaust velocity of particles in Hall thrusters is much lower than the speed of light:

$$v_{\text{ex}} \ll c. \tag{2.1}$$

2.1 FUNDAMENTALS OF ELECTROMAGNETISM

When describing electric propulsion engine, we need to know about fundamental physics enabling the engine to work. Only most needed fundamentals will be covered. If reader wants to read more, additional information can be found in [3], [8] or [9].

Coulomb force is describing interaction between particles or point charges, visualized in figure 2.1 and written as

$$\mathbf{F}_{\text{C}}(\mathbf{r}) = \frac{1}{4\pi\epsilon_0} \frac{Q_{\text{p}}q}{\|\mathbf{r} - \mathbf{r}'\|^3} \cdot (\mathbf{r} - \mathbf{r}'), \tag{2.2}$$

Figure 2.1: Coulomb force acting between two particles.

However, for our case, we need the description of the electric field that is accelerating particles. We can define this electric field as *electric intensity*:

$$\mathbf{E}(\mathbf{r}) = \frac{\mathbf{F}_{\mathrm{C}}}{Q_{\mathrm{p}}} = \frac{1}{4\pi\epsilon_0} \frac{q}{\|\mathbf{r} - \mathbf{r}'\|^3} \cdot (\mathbf{r} - \mathbf{r}'). \tag{2.3}$$
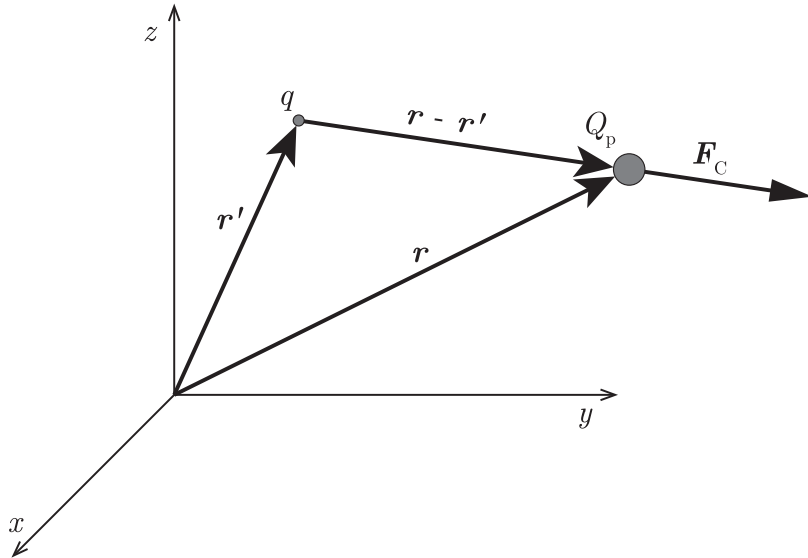
We clearly see that electric intensity is describing *imaginary points*, at which (when added testing charge) field would create acting force of certain value. Reason why electric intensity is introduced is because of the fact that various forms of electric field exist, where electric field produced by Coulomb force is only one of many. Electric intensity can be also obtained as

$$\mathbf{E}(\mathbf{r}) = -\boldsymbol{\nabla}\phi(\mathbf{r}), \tag{2.4}$$

where ϕ is potential at vector $\mathbf{r}$. Potential is allowing us to relate intensity of electric field to any object with a given charged surface. Minus sign is due to the fact that particles have tendency to move along the path heading to the minimum of potential energy. It tells us that electron moves towards higher electric potential and that positively charged particles will move further away from this field, as we will experience and discuss this phenomena in following chapters. This potential is defined as

$$\phi(\mathbf{r}) = \frac{1}{4\pi\epsilon_0} \frac{q}{\|\mathbf{r} - \mathbf{r}'\|}. \tag{2.5}$$

For establishing conclusions and being able to calculate power and energy of Hall thruster and electromagnetic fields present, we need to define potential energy and power. Close relation exists between potential energy and the *work done*, where work done along random path C is

$$W_{\mathrm{p}}(C) = Q_{\mathrm{p}} \int_{\mathbf{r}_0}^{\mathbf{r}} \mathbf{E}(\mathbf{r}') \cdot d\mathbf{r}'. \tag{2.6}$$

Potential energy is energy of particle Q in a random position $\mathbf{r}$. This energy may or may not be the same as work done, depending on situation. In general case, *potential energy* of particle Q in position $\mathbf{r}$ is

$$\mathcal{V}_{\mathrm{p}}(\mathbf{r}) = Q_{\mathrm{p}}\phi(\mathbf{r}). \tag{2.7}$$

If particle did not possess any energy at the start, it will gain energy equal to work electric field had to release to move particle from position $\mathbf{r}_0$ to $\mathbf{r}$. This work can be characterized by equation (2.6) or with use of equation (2.4) as potential difference between two points multiplied by charge of particle, and declared to be the new potential energy of particle as

$$W_{\mathrm{p}} = Q_{\mathrm{p}} \int_{\mathbf{r}}^{\mathbf{r}_0} \boldsymbol{\nabla}\phi(\mathbf{r}') \cdot d\mathbf{r}' = Q_{\mathrm{p}} \int_{\phi(\mathbf{r})}^{\phi(\mathbf{r}_0)} d\phi = Q_{\mathrm{p}}(\phi(\mathbf{r}_0) - \phi(\mathbf{r})) = Q_{\mathrm{p}}U = \mathcal{V}_{\mathrm{p}}, \tag{2.8}$$

where U is *potential difference* between positions $\mathbf{r}_0$ and $\mathbf{r}$. This equation will be very important, as it brings together relation between charge of particle and potential difference, which will be essential. This energy is equal to kinetic energy particle gains while moving from position $\mathbf{r}_0$ to $\mathbf{r}$, mathematically written as

$$\mathcal{T}_{\mathrm{p}} = \frac{1}{2}m_{\mathrm{p}} \left(\|\mathbf{v}_{\mathrm{p}\mathbf{r}}\|^2 - \|\mathbf{v}_{\mathrm{p}\mathbf{r}_0}\|^2 \right). \tag{2.9}$$

Derivations of this relations are not part of this work, however the most important ones were presented. For more information look in [3] or any other physics book.

2.2 FORCES, ION AND ELECTRON MOVEMENT

Electrons and ions share the same charge, only with opposite polarity. The reason is in ionization process, when ions (or cations - to be accurate) are created. They are disposed mostly of one electron, which makes them positively charged by the exact amount of charge they lost. It happens that ions have double charge, because two electrons from atomic shell were extracted, however we will reckon on single charged ions only, as double charged are not that frequent.

Ions are accelerated electrostatically, which means that they feel the force acting on them:

$$\mathbf{F}_\mathrm{i} = Q\mathbf{E}. \tag{2.10}$$

This is the main force that is causing spacecraft to move forward, however not the only one acting on ions. Magnetic field present also affects these ions. Previous equation then becomes

$$\mathbf{F}_\mathrm{i} = Q\mathbf{E} + Q(\mathbf{v}_i \times \mathbf{B}), \tag{2.11}$$

where $\mathbf{v}_\mathrm{i}$ is velocity vector of ion that is being accelerated. One might ask if it is desirable behavior, when the very same field traps electrons that gyrate around the discharge chamber. Indeed, it actually is undesirable, but it does not affect the ions in a degree that would make the engine to fail. The key is mass of ions, that are (in case of xenon), approximately 2.3698×10^5 heavier then electrons. This fact implies that magnetic field must be designed in such a way that it traps electrons, but not ions. Despite of this, ions are still slightly affected, which results in a minor rotation around acceleration axis.

Electrons experience the same forces as ions, but their behavior is highly different. As they are much smaller, they are trapped by the magnetic field, which means that they cannot move in direction of acceleration axis by a great amount. Force acting on electrons is

$$\mathbf{F}_\mathrm{e} = -Q\mathbf{E} - Q(\mathbf{v}_\mathrm{e} \times \mathbf{B}). \tag{2.12}$$

Velocity of electron $\mathbf{v}_\mathrm{e}$ is defined as

$$\mathbf{v}_\mathrm{e} = \frac{\mathbf{E} \times \mathbf{B}}{B^2}, \tag{2.13}$$

with magnitude

$$v_\mathrm{e} = \frac{\|\mathbf{E} \times \mathbf{B}\|}{B^2} = \frac{E \overbrace{\|\hat{\mathbf{E}} \times \hat{\mathbf{B}}\|}^{=\sin(\theta_\mathrm{EB})} B}{B^2} = \frac{E}{B}\sin(\theta_\mathrm{EB}). \tag{2.14}$$

Electron velocity with its elementary charge density creates *current density*, also called *Hall current density*:

$$\mathbf{j}_\mathrm{Hall} = -\rho\mathbf{v}_\mathrm{e}, \tag{2.15}$$

where

$$\rho = \lim_{\Delta V \to 0} \frac{Q}{\Delta V}. \qquad (2.16)$$

We will assume that ionized plasma is quasi–neutral, which menas that

$$Qn_{\mathrm{i}} \approx Qn_{\mathrm{e}}. \qquad (2.17)$$

Combination of equations (2.11), (2.15) and (2.17) refers to

$$\mathbf{F}_{\mathrm{i}} = Q\mathbf{E} - \iiint\limits_{V} (\mathbf{j}_{\mathrm{Hall}} \times \mathbf{B})dV = 2\pi \iint\limits_{S_{\mathrm{rz}}} (\mathbf{j}_{\mathrm{Hall}} \times \mathbf{B})rdrdz, \qquad (2.18)$$

where r is radius we are integrating on and z is height of discharge chamber.

Electrons feel much more complicated acting forces than the $\mathbf{E} \times \mathbf{B}$ drift or acceleration from electric field. Their motion is considerably complicated. For instance, due to electric field, electrons are pulled down, then reflected near the bottom (or even upper) core of the magnet. They are gyrating around the discharge chamber due to $\mathbf{E} \times \mathbf{B}$ drift, but they also feel drifts like $\boldsymbol{\nabla}B$ drift – due to the change of magnetic field, then curvature drift, where nothing more than centripetal force is the primary cause. Even gravitational drift may take into account, but only when engines are ground tested at research facilities. Possible motion of electron is shown in figure 2.2.
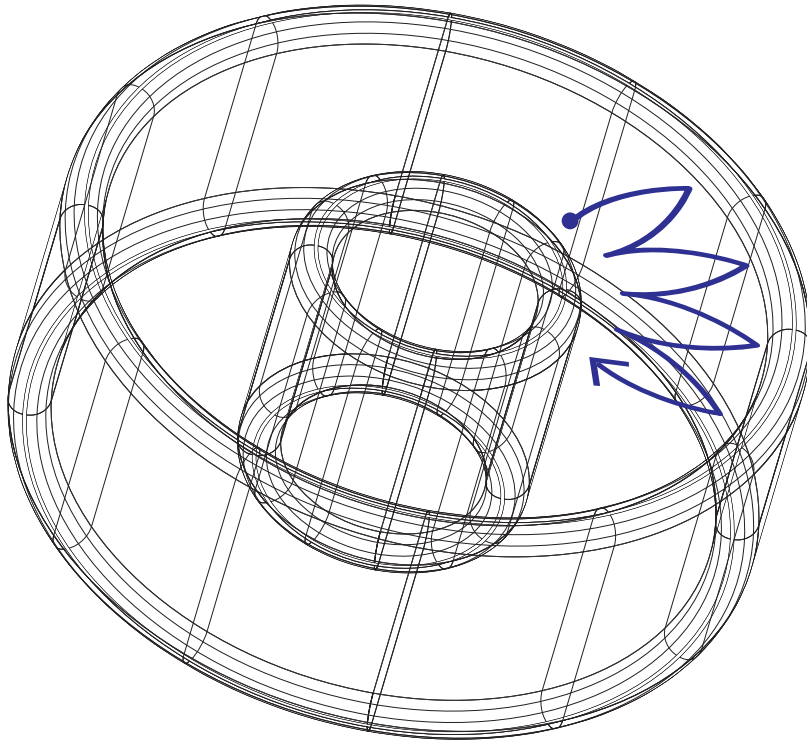

Figure 2.2: Gyrating motion of electron around discharge chamber.

2.3 RELATIVISTIC EQUATIONS

Generally, in theory of ion propulsion engines, use of relativistic equations is not needed because ions don't have the time to be accelerated to any significantly large velocity value that is close to the speed of light. We will however simulate also motion of electrons, which posses huge difference in their mass, if compared to ions. This difference allows them to significantly increase their velocity, in few cases to the limit of 10^7 m/s or even higher, where relativity is notable. That is the reason why we will cover simplified derivations of relativistic equations.

Momentum of electron for relativistic case is defined as

$$\mathbf{p}_e = \gamma m_{e_0} \mathbf{v}_e + Q\mathbf{A}, \tag{2.19}$$

where

$$\gamma = \frac{1}{\sqrt{1 - \frac{\mathbf{v}_e^2}{c^2}}}, \tag{2.20}$$

and m_{e_0} stands for normal mass of electron (real mass of electron, not influenced by relativistic conditions). We did include vector potential $\mathbf{A}$ for integrity, however it is useful only in Hamilton equations. If we omit this potential, our final equation for momentum is

$$\mathbf{p}_e = \gamma m_{e_0} \mathbf{v}_e. \tag{2.21}$$

We can substitute this equation into definition of Lorentz force, which yields to

$$\frac{d\mathbf{p}_e}{dt} = m_{e_0} \frac{d}{dt} \left(\frac{\mathbf{v}_e}{\sqrt{1 - \frac{\mathbf{v}_e^2}{c^2}}} \right) = -Q\mathbf{E} - Q(\mathbf{v}_e \times \mathbf{B}). \tag{2.22}$$

After initial derivation, equation is

$$m_{e_0} \frac{\dot{\mathbf{v}}_e \sqrt{1 - \frac{\mathbf{v}_e^2}{c^2}} + \frac{\mathbf{v}_e^2}{c^2 \sqrt{1 - \frac{\mathbf{v}_e^2}{c^2}}} \dot{\mathbf{v}}_e}{1 - \frac{\mathbf{v}_e^2}{c^2}} = -Q\mathbf{E} - Q(\mathbf{v}_e \times \mathbf{B}). \tag{2.23}$$

Determined reader can complete the derivation himself, however the result is

$$m_{e_0} \dot{\mathbf{v}}_e = \alpha[-Q\mathbf{E} - Q(\mathbf{v}_e \times \mathbf{B})], \tag{2.24}$$

where we marked α as

$$\alpha = \frac{c^2 \left(1 - \frac{\mathbf{v}_e^2}{c^2}\right)^2}{\sqrt{1 - \frac{\mathbf{v}_e^2}{c^2}} \left[c^2 \left(1 - \frac{\mathbf{v}_e^2}{c^2}\right) + \mathbf{v}_e^2\right]}. \tag{2.25}$$

Relativistic equation for ions would be

$$m_{i_0} \dot{\mathbf{v}}_i = \alpha[Q\mathbf{E} + Q(\mathbf{v}_i \times \mathbf{B})]. \tag{2.26}$$

2.4 THRUST

Main element creating thrust are ions, which can be taken into account as a stream of ions, called *ion beam*, or each ion individually. This work discusses about particle motion, so our main interest are individual particles as ions and electrons, however final conclusions would have to be created for ion beams, as only in this way engine actually produces noticeable thrust.

Thrust of a single ion is equal to opposite of what ion feel, mathematically:

$$\mathbf{T}_i = -\mathbf{F}_i. \tag{2.27}$$

Component that forces vehicle to move forward is scalar value only in z - direction, written as

$$[\mathbf{T}_i]_z = \|\mathbf{T}_i\| \sin(\theta). \tag{2.28}$$

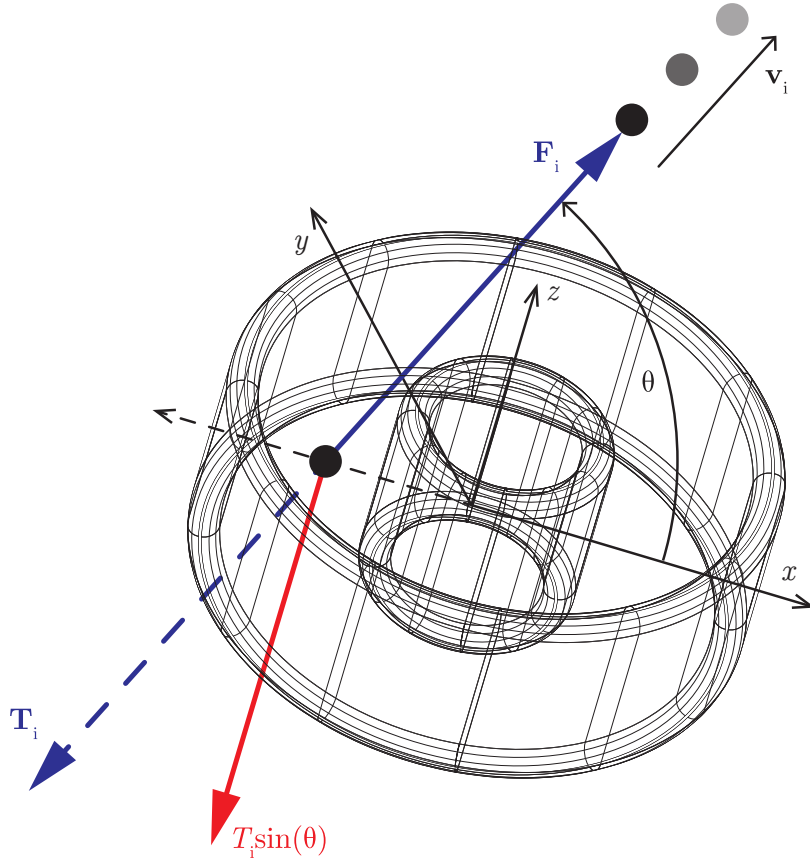and shown in figure 2.3:

Figure 2.3: Thrust produced by a single ion.

While for simulations are individual particles essential, for discussing engine power and similar properties, we have to define thrust of all particles producing thrust combined. Thrust generated by ion beam can be derived as

$$T = \sum_{k=1}^{N_i} \|\mathbf{T}_{i_k}\| \sin(\theta) = N_i \|\mathbf{T}_i\| \sin(\theta). \tag{2.29}$$

Another way of defining thrust that is more useful from perspective in which we don't know what is the force acting on every single ion, can be written as

$$T = \frac{d}{dt}(m_{\mathrm{ppl}}v_{\mathrm{ex}}) = \dot{m}_{\mathrm{ppl}}v_{\mathrm{ex}}, \tag{2.30}$$

where v_{ex} is *actual exhaust velocity* (constant value) and m_{ppl} is *propellant mass*. It is important to note that thrust generated is not the same as thrust generated by ions, however it is extremely close. Reason for this is due to the fact that velocity of ions greatly exceeds velocity of anything else that contributes to thrust production. Mathematically speaking:

$$\dot{m}_{\mathrm{ppl}}v_{\mathrm{ex}} \approx \dot{m}_{\mathrm{ions}}v_{\mathrm{ions}}, \tag{2.31}$$

where m_{ions} is mass of all of the ions combined

$$m_{\mathrm{ions}} = \sum_{k=1}^{N_{\mathrm{i}}} m_{\mathrm{i}_k} = N_{\mathrm{i}}m_{\mathrm{i}}, \tag{2.32}$$

and change of ion mass over time is

$$\dot{m}_{\mathrm{ions}} = \mathcal{N}_{\mathrm{i}}m_{\mathrm{i}}, \tag{2.33}$$

where $\mathcal{N}_{\mathrm{i}}$ is flow of ions per second. We can now continue in computations, neglecting unnoticeable effects of other particles such as electrons and non–ionized, neutral particles of propellant.

Kinetic energy of specific mass of the ion beam in a given time stamp is

$$\mathcal{T}_{\mathrm{ions}} = \frac{1}{2}m_{\mathrm{ions}}v_{\mathrm{ions}}^2. \tag{2.34}$$

Power of this ion beam is characterized as

$$P_{\mathrm{ions}} = \frac{d\mathcal{T}_{\mathrm{ions}}}{dt} = \frac{d}{dt}\left(\frac{1}{2}m_{\mathrm{ions}}v_{\mathrm{ions}}^2\right) = \frac{1}{2}\dot{m}_{\mathrm{ions}}v_{\mathrm{ions}}^2. \tag{2.35}$$

If we now substitute equation (2.30) into equation above, with corrections from equation (2.31), relation we get is

$$P_{\mathrm{ions}} = \frac{1}{2}Tv_{\mathrm{ions}} = \frac{T^2}{2\dot{m}_{\mathrm{ions}}} = \frac{T^2}{2\mathcal{N}_{\mathrm{i}}m_{\mathrm{i}}} \approx P_{\mathrm{jet}}, \tag{2.36}$$

where P_{jet} is total power of the ion engine that is needed for nominal operation.

Moving ions create current while moving through given area. Total work of all ions gained while flowing through two separate positions of different potentials, but mostly the energy released by ion engine to move all of these ions by given distance, can be written as

$$W_{\mathrm{ions}} = U\sum_{k=1}^{N_{\mathrm{i}}} Q_k = N_{\mathrm{i}}UQ. \tag{2.37}$$

Current generated by a single ion is

$$I = \frac{dQ}{dt}. \tag{2.38}$$

Time derivation of equation (2.37) gives

$$\frac{dW_{\text{ions}}}{dt} = N_{\text{i}}U\frac{dQ}{dt} = N_{\text{i}}UI = P_{\text{ions}}, \tag{2.39}$$

which is well-known equation for electric power. Comparing this equation with equation (2.35) gives

$$UN_{\text{i}}I = \frac{T^2}{2\mathcal{N}_{\text{i}}m_{\text{i}}} \implies T = \sqrt{2\mathcal{N}_{\text{i}}N_{\text{i}}UIm_{\text{i}}}. \tag{2.40}$$

From this equation, we can clearly see that increasing mass of ions (choosing gas with heavier atoms), increasing density of ions, potential between two separate positions (in our case – distance from anode and cathode) or changing the charge of every ion (detaching more electrons) will greatly affect output thrust generated, which is – frankly speaking – logical, isn't it?

The same can be applied for electrons. Flow of electrons would define power generated by ion engine itself, as they are the ones that close the electric circuit. Power generated by engine is in ideal case equal to power of ions, thus describes efficiency of the engine.

2.5   SPECIFIC IMPULSE AND ROCKET EQUATION

Specific impulse is very important, as it is main characteristic of every rocket engine. It is a ratio of thrust produced to the rate of propellant consumption [4]. Specific impulse for constant thrust and mass flow rate is

$$I_{\text{sp}} = \frac{T}{\dot{m}g}, \tag{2.41}$$

where $\dot{m}$ is change of spacecraft's mass over time and g is gravitational acceleration at ground level. The fact that we are calculating with the mass of whole spacecraft doesn't matter. Of course, mass of spacecraft is a lot different compared to mass of propellant, which in our case may be just few kilograms of xenon gas. Mass change rate however, stays the same, because propellant is the only element that is actually being consumed, therefore

$$\dot{m} = \dot{m}_{\text{ppl}}. \tag{2.42}$$

Combination of equation (2.30) with equation (2.41) yields to

$$I_{\text{sp}} = \frac{v_{\text{ex}}}{g}, \tag{2.43}$$

After this introduction, we can interpret specific impulse as the time which will increase spacecraft's *delta–v* by a specific value with engine continuously functioning in optimal

conditions, where delta–v is formerly known as change in velocity needed to perform various tasks. This can be written as

$$\Delta v = \int\limits_{t_{\text{init}}}^{t_{\text{final}}} \frac{T}{m} dt. \tag{2.44}$$

With use of equation (2.30), we can write

$$\Delta v = \int\limits_{t_{\text{init}}}^{t_{\text{final}}} v_{\text{ex}} \frac{\dot{m}}{m} dt = - \int\limits_{m}^{m-m_{\text{ppl}}} v_{\text{ex}} \frac{dm}{m} = \int\limits_{m-m_{\text{ppl}}}^{m} v_{\text{ex}} \frac{dm}{m}, \tag{2.45}$$

where we used the fact that reduction of mass of the vehicle over time is negative to mass that comes into the nozzle, or combustion chamber of engine. Previous equation can be integrated into

$$\Delta v = v_{\text{ex}} \ln \left(\frac{m}{m - m_{\text{ppl}}} \right), \tag{2.46}$$

which is famous and well–known **ideal rocket equation**, found by Konstantin Tsiolkovsky.

These equations will be used in following chapters, when we will attempt to describe theoretical properties of Hall effect ion engine.

CHAPTER 3
ELECTRIC AND MAGNETIC FIELDS

For purposes of simulations, we have to design electric and magnetic field. This thesis, as was said earlier, does not want to cover the details of designing a Hall Ion Thruster. However, even in purely theoretical way, to observe mentioned motion of particles, we are obliged to have certain properties of electric and magnetic field. While doing so, there rises a question, why not to design relatively closed approximation of a realistic electromagnetic field present? This chapter will cover this problem.

3.1   DISCHARGE CHAMBER

First of all, we have to design the theoretical shape of discharge chamber and layout of magnets producing magnetic dipoles. As shown in introduction, discharge chamber is of annular shape, with core electromagnet in its center. Surface of the anode, located on the bottom of discharge chamber and also layout of magnets is shown in figure 3.1.
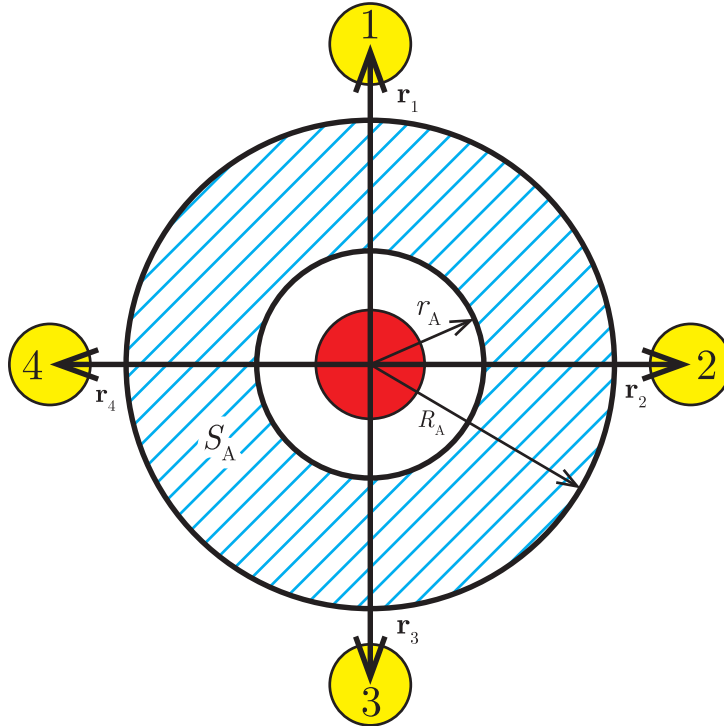

Figure 3.1: Surface of anode at the bottom of discharge chamber.

Surface area of the anode is

$$S_\mathrm{A} = \iint\limits_{S_\mathrm{A}} r\,dr\,d\varphi = 2\pi \int\limits_{r_\mathrm{A}}^{R_\mathrm{A}} r\,dr = \pi(R_\mathrm{A}^2 - r_\mathrm{A}^2). \tag{3.1}$$

Ion thrusters are being designed in various sizes, however mostly doesn't exceed few dozens of centimeters in diameter. Few thrusters were designed by NASA with diameter of 500 millimeters, but not more. Most of the designs are quite small. We will focus on a design with 200 millimeters in diameter, written as

$$R_\mathrm{A} = 100 \text{ mm}, \tag{3.2}$$

where R_A is major radius of discharge chamber from figure 3.1. Minor radius r_A is essential from mechanical perspective, however in our case it is not necessary, yet we will define it as:

$$r_\mathrm{A} = 50 \text{ mm}. \tag{3.3}$$

Vectors for magnetic dipole positions are

$$\mathbf{r}_c = (0, 0, 60) \text{ mm}, \tag{3.4}$$
$$\mathbf{r}_1 = (0, 140, 60) \text{ mm}, \tag{3.5}$$
$$\mathbf{r}_2 = (140, 0, 60) \text{ mm}, \tag{3.6}$$
$$\mathbf{r}_3 = (0, -140, 60) \text{ mm}, \tag{3.7}$$
$$\mathbf{r}_4 = (-140, 0, 60) \text{ mm}. \tag{3.8}$$

3.2   ELECTRIC FIELD

Closest approximation of electric field would be formula for electric field of a charged plate. If we slightly adjust the formula for surface S_A, from *Gauss Law* we get

$$\oiint\limits_{S'} E_\mathrm{A}\,dS \approx \frac{q}{\epsilon_0}, \tag{3.9}$$

where S' is theoretical and symmetrical surface surrounding the surface S_A. Note that the value is only an approximation of this law, because it would be equal only for charged plate of infinite dimensions. From previous equation, we can obtain

$$E_\mathrm{A} \approx \frac{q}{2\epsilon_0 S'} = \frac{\sigma}{2\epsilon_0}, \tag{3.10}$$

where σ is surface density of charge q built on area of surface S':

$$\sigma = \frac{q}{S'}. \tag{3.11}$$

Since electric field consists of anode and cathode, where cathode is so called virtual cathode created by gyrating electrons, electric intensity for our case would be

$$E = E_\mathrm{A} - E_\mathrm{C}, \tag{3.12}$$

where E_C is electric intensity of cathode labeled

$$E_C \approx \begin{cases} -\dfrac{\sigma}{2\epsilon_0}. & 0 \leq d_C \leq \text{height of chamber}, \\ \dfrac{\phi_C}{d_C} & d_C > \text{height of chamber}, \end{cases} \tag{3.13}$$

where ϕ_C is potential of cathode and d_C is distance from cathode. Our final vector of electric intensity **inside** of discharge chamber which is oriented in z direction is:

$$\mathbf{E} \approx \frac{\sigma}{\epsilon_0}\hat{\mathbf{r}}_z. \tag{3.14}$$

Note that this intensity is (after evaluation) a constant number. This fact is very important, because it tells us that we are able to approximate electric field inside the discharge chamber as a simple one-directional homogeneous field. Visualization of this field is shown in figure 3.2.
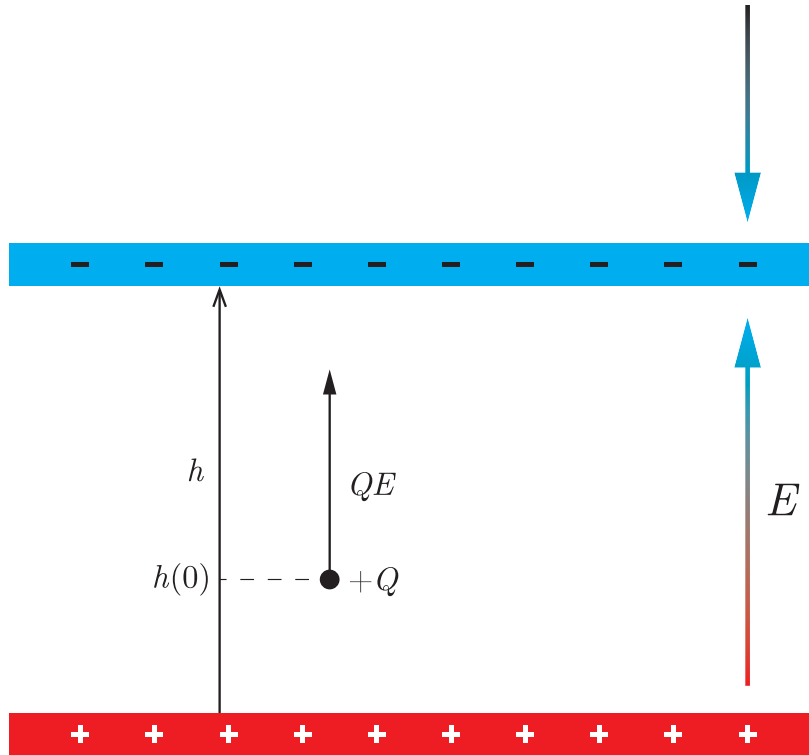
Figure 3.2: Electric field inside and outside of discharge chamber.

We see that electric field from cathode could be a major problem, since it could decelerate ions that were previously accelerated. This is however not true, because ions are neutralized after passing gyrating electrons, or after binding with free electrons emitted from cathode. Even if they wouldn't, electric field outside of discharge chamber would rapidly lower its magnitude with every increased distance from it.

For evaluation of intensity from equation (3.14), we have to know potential difference

U between anode and cathode and use formula

$$E = \frac{U}{d_{\mathrm{AC}}}, \tag{3.15}$$

where d_{AC} is distance between anode and cathode. Dimensions such as diameter and height of discharge chamber (d_{AC}) come from experimental data achieved, as was said in introduction, mainly by Russian scientists in 1960s. These data say that heigh of discharge chamber should be half of its diameter or slightly lower. We can define our as

$$d_{\mathrm{AC}} = 80 \text{ mm}. \tag{3.16}$$

Potential difference can be calculated as:

$$U = \phi_{\mathrm{A}} - \phi_{\mathrm{C}}, \tag{3.17}$$

therefore, we have to obtain potentials of anode and cathode. Let potential of anode be 1000 V, that is somehow a reasonable value, possible in real world applications, written as:

$$\phi_{\mathrm{A}} = 1000 \text{ V}. \tag{3.18}$$

Potential of cathode is tricky part, since we are basically discussing potential created by moving point charges - electrons. This is the part of a problem where knowledge is based purely by experiments. As while writing this thesis I was not able to obtain any realistic data providing how large values should the built potential from electrons achieve, we have to deduce this by pure logic and experimentation, which will be done in chapter 5 where we will focus more on simulations.

The only aspect we have to know is how many electrons could be gyrating around discharge chamber. *Avogadro constant* N_{A} describes how many atoms, molecules, or any combination of particles can be located in 1 mol. This number is $N_{\mathrm{A}} = 6.02214129(27) \times 10^{23}$ mol^{-1}. All of our simulations will be done for stable isotope of xenon $^{130}_{54}$Xe with molar mass of approximately 130 g/mol, which means that 130 g of xenon $^{130}_{54}$Xe will roughly contain number of atoms equal to Avogadro constant. We know that ions are built by ionization and by insertion of electrons from hot electrode. In the process of ionization, one electron is detached, creating approximately $6.02214129 \times 10^{23}$ electrons from 130 g of xenon. This is, however, a little bit too much. If we reduce this number, for initial simulations, to 10^{10} electrons, we can obtain potential of cathode by approximation of formula

$$\phi_{\mathrm{C}} = -\sum_{k=1}^{10^{10}} \frac{1}{4\pi\epsilon_0} \frac{Q_k}{d_{\mathrm{AC}}} \approx -179.9956 \text{ V}. \tag{3.19}$$

Combination of equations (3.17), (3.18) and (3.19) yields to our initial potential difference between anode and cathode, which is

$$U \approx 1180 \text{ V}. \tag{3.20}$$

Finally, with use of equation (3.15) and (3.14), we obtain vector of electric field

$$\mathbf{E} = (0, 0, 14750) \text{ V/m}. \tag{3.21}$$
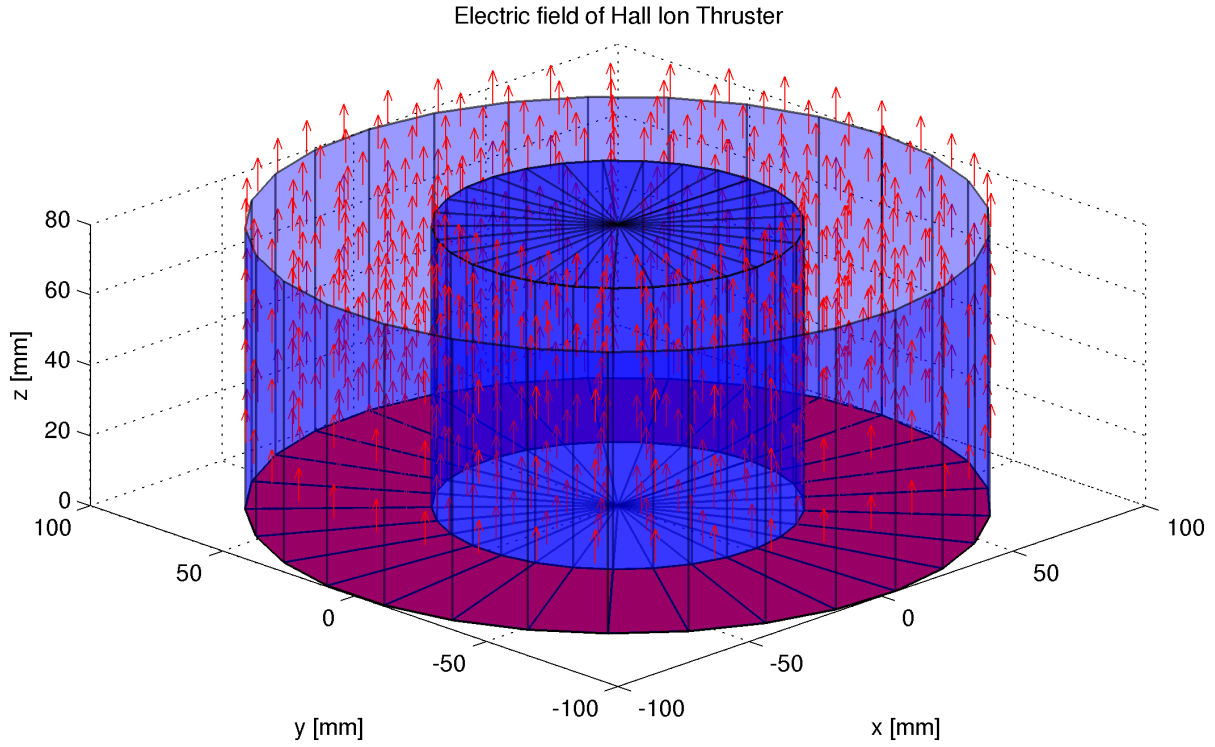
Electric field of Hall Ion Thruster

Figure 3.3: Visualization of electric field inside discharge chamber.

Visualization of discharge chamber and electric field $\mathbf{E}$ inside is in figure 3.3.

Very important relization now should come into mind. **Ions feel potential difference of anode and cathode**, therefore they are being accelerated by electric field described in equation (3.21). **Electrons** are, however, producers of this imaginary cathode, which means they **feel only electric field of anode**, not both anode and cathode. Vector of electric field produced only by anode is

$$\mathbf{E}_{\mathrm{A}} = \frac{\phi_{\mathrm{A}}}{d_{\mathrm{AC}}} \hat{\mathbf{r}}_{\mathrm{z}} = (0, 0, 12500) \ \mathrm{V/m}. \tag{3.22}$$

3.3 MAGNETIC FIELD

In real application of Hall effect ion thruster, superconductive magnets, created by coils would be used. Magnetic field of a coil is not necessary when discussing theory of particle motion. It is true that for further research, this magnetic field would have to be used, however for our current situation magnetic dipole is sufficient, needless to say that magnetic field of coil is only slightly more complicated than its predecessor - magnetic dipole.

Magnetic dipole is created by a closed loop of current with specific magnitude. This current is characterized by *magnetic dipole moment*, defined as

$$\|\mathbf{p}_{\mathrm{M}}\| = \left\| \frac{1}{2} Q_{\mathrm{p}} (\mathbf{r}_{\mathrm{p}} \times \mathbf{v}_{\mathrm{p}}) \right\| = \frac{m_{\mathrm{p}} v_{\perp}^2}{2E} = IS', \tag{3.23}$$

where S' is section surface of the coil. For magnetic dipole oriented in z direction, this vector is

$$\mathbf{p}_\mathrm{M} = (0, 0, p_\mathrm{M}). \tag{3.24}$$

With knowledge of magnetic dipole moment, we are able to create vector potential:

$$\mathbf{A} = \frac{\mu_0}{4\pi} \frac{\mathbf{p}_\mathrm{M} \times \mathbf{r}}{\|\mathbf{r}\|^3}, \tag{3.25}$$

from which magnetic field is easily derived as

$$\mathbf{B} = \boldsymbol{\nabla} \times \mathbf{A} = \frac{\mu_0}{4\pi} \frac{3(\mathbf{p}_\mathrm{M} \cdot \mathbf{r})\mathbf{r} - \|\mathbf{r}^2\|\mathbf{p}_\mathrm{M}}{\|\mathbf{r}\|^5}. \tag{3.26}$$

For magnetic dipole oriented in z direction, we get

$$\mathbf{A} = \frac{\mu_0}{4\pi} \frac{(-y, x, 0)}{\|\mathbf{r}^3\|}, \tag{3.27}$$

$$\mathbf{B} = \|\mathbf{p}_\mathrm{M}\| \frac{\mu_0}{4\pi} \frac{(3xz, 3yz, -x^2 - y^2 + 2z^2)}{\|\mathbf{r}^5\|}. \tag{3.28}$$

Since we are not using *Hamilton equations* for derivation of differential equations, but rather direct solution with Lorentz force, magnetic field $\mathbf{B}$ is our primary object of focus.

At the beginning, we will focus on magnetic field that consists of core magnet and 4 slave magnets, as shown in figure 1.5. Magnetic field of core magnet is

$$\mathbf{B}_\mathrm{c} = \|\mathbf{p}_{\mathrm{M}_\mathrm{c}}\| \frac{\mu_0}{4\pi} \frac{(3xz_{\mathrm{off}_\mathrm{c}}, 3yz_{\mathrm{off}_\mathrm{c}}, -x^2 - y^2 + 2z_{\mathrm{off}_\mathrm{c}}^2)}{\|\mathbf{r} - \mathbf{r}_\mathrm{c}\|^5}, \tag{3.29}$$

where

$$z_{\mathrm{off}_\mathrm{c}} = z - z_\mathrm{c}, \tag{3.30}$$

$$\mathbf{r}_\mathrm{c} = (0, 0, z_\mathrm{c}). \tag{3.31}$$

Semi–fields of supportive magnets can be written as

$$\mathbf{B}_\mathrm{j} = \|\mathbf{p}_{\mathrm{M}_\mathrm{j}}\| \frac{\mu_0}{4\pi} \frac{(3x_{\mathrm{off}_\mathrm{j}} z_{\mathrm{off}_\mathrm{j}}, 3y_{\mathrm{off}_\mathrm{j}} z_{\mathrm{off}_\mathrm{j}}, -x_{\mathrm{off}_\mathrm{j}}^2 - y_{\mathrm{off}_\mathrm{j}}^2 + 2z_{\mathrm{off}_\mathrm{j}}^2)}{\|\mathbf{r} - \mathbf{r}_\mathrm{j}\|^5}, \quad j = 1, 2, 3, 4, \tag{3.32}$$

where

$$x_{\mathrm{off}_\mathrm{j}} = x - x_\mathrm{j}, \tag{3.33}$$

$$y_{\mathrm{off}_\mathrm{j}} = y - y_\mathrm{j}, \tag{3.34}$$

$$z_{\mathrm{off}_\mathrm{j}} = z - z_\mathrm{j}, \tag{3.35}$$

$$\mathbf{r}_\mathrm{j} = (x_\mathrm{j}, y_\mathrm{j}, z_\mathrm{j}). \tag{3.36}$$

Resulting magnetic field is

$$\mathbf{B} = \mathbf{B}_\mathrm{c} + \sum_{j=1}^{4} \mathbf{B}_\mathrm{j} = \mathbf{B}_\mathrm{c} = \|\mathbf{p}_{\mathrm{M}_\mathrm{c}}\| \frac{\mu_0}{4\pi} \frac{(3xz_{\mathrm{off}_\mathrm{c}}, 3yz_{\mathrm{off}_\mathrm{c}}, -x^2 - y^2 + 2z_{\mathrm{off}_\mathrm{c}}^2)}{\|\mathbf{r} - \mathbf{r}_\mathrm{c}\|^5} +$$

$$+ \|\mathbf{p}_{\mathrm{M}_\mathrm{j}}\| \frac{\mu_0}{4\pi} \sum_{j=1}^{4} \frac{(3x_{\mathrm{off}_\mathrm{j}} z_{\mathrm{off}_\mathrm{j}}, 3y_{\mathrm{off}_\mathrm{j}} z_{\mathrm{off}_\mathrm{j}}, -x_{\mathrm{off}_\mathrm{j}}^2 - y_{\mathrm{off}_\mathrm{j}}^2 + 2z_{\mathrm{off}_\mathrm{j}}^2)}{\|\mathbf{r} - \mathbf{r}_\mathrm{j}\|^5}. \tag{3.37}$$

Previous equations allow us to move all of the four slave magnets around discharge chamber freely, positioning them anywhere in x, y and z direction, with core magnet in their center, positioned freely only in z direction.

Vector of magnetic field allows us to describe the behavior of this field, however we still have to specify its strength. There is no preferred way for this particular problem, where the most effective is just an experimental trial-and-error method, yet there still may exist calculation that allows us to feel the strength of field just in a little tiny bit. We are able to create gradient vector of magnitude of vector field described by equation (3.37), noted as

$$\boldsymbol{\nabla} B = \frac{\mathrm{D}B}{\mathrm{D}(x,y,z)}, \tag{3.38}$$

where we want to focus particularly on radial direction, which means to fix x or y variable and look on the other as constants. If we focus, for example, on y direction, we are able to created function of strength of magnetic field that is equal to zero, noted as

$$f_{\mathrm{B}}(y_0) = \frac{\partial B}{\partial y} \overset{!}{=} 0. \tag{3.39}$$

We clearly see that the equation above represents slope of straight line with constant value in stationary point y_0, that is tangential to function of magnetic field $B(x, y_0, z)$ – thus finding local extreme in this point, representing local minimum of strength of magnetic field. Final relation of this equation would be connection between stationary point, local minimum and strength of magnetic dipole moments $p_{\mathrm{M_c}}$ and $p_{\mathrm{M_j}}$, where $j = 1, 2, 3, 4$. With this result we could find optimal position y_0 of place with lowest energy, located on y axis, where electrons would posses the most efficient location for gyrating motion. This position would be highly influenced by magnetic dipole moments, which would allow us to find the optimal relation between dipole moment of core magnet and dipole moments of the other four. In conclusion – we've got this option or the experimental one, where we have to choose wisely. Looking at magnificent shape of equation (3.37), we swiftly and unnoticed move to experimental result, where position representing least of magnetic field strength lies roughly in

$$y_0 \approx 0.075 \ m. \tag{3.40}$$

Interesting thing to observe is the fact that this value is in exact center between inner walls of discharge chamber, creating *central line* with set of points defined as

$$O = \left\{ \forall (\rho, \varphi) \in \mathbb{R}^2 : \rho = \frac{R_{\mathrm{A}} + r_{\mathrm{A}}}{2} = 0.075 \wedge \varphi \in (0, 2\pi) \right\}, \tag{3.41}$$

which is shown in figure 3.4.

Since electrons enter the chamber by emission from cathode, we want to set our field approximately few millimeters above discharge chamber. This value was experimentally proven to be 30 millimeters. As shown in figure 3.4, we want the x axis to be fixed, thus equal to zero. Following previous derivations, vector representing position of place where we are trying to find nominal value of magnetic field is

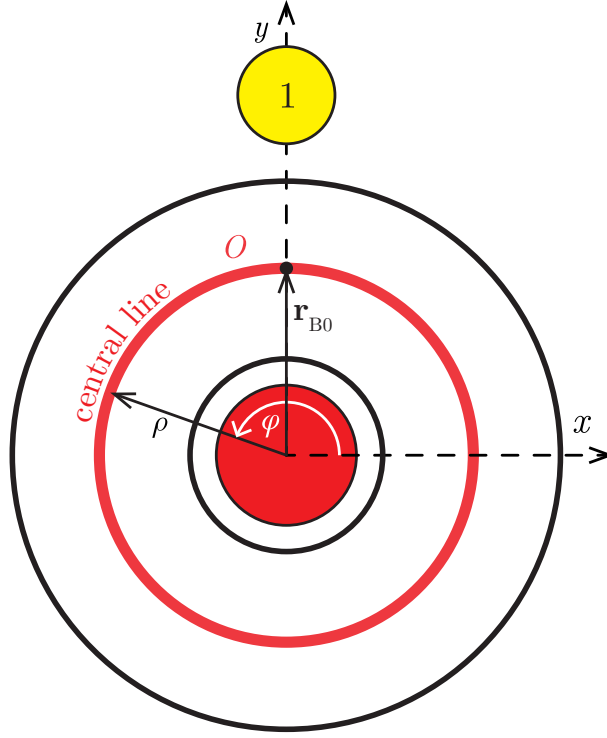$$\mathbf{r}_{\mathrm{B_0}} = (0, 75, 90) \ \mathrm{mm}. \tag{3.42}$$

Figure 3.4: Central line of discharge chamber.

Note that by rotating this vector around discharge chamber azimuthally, we are able to create radial field line representing points with (roughly) the same value of magnetic field. Strength of this field was experimentally proven fact mainly by Russian and American scientist in past decade. Based on [6], we can define our strength of magnetic field in position $\mathbf{r}_{B_0}$ as

$$\mathbf{B}(\mathbf{r}_{B_0}) = 0.0554 \text{ T}, \tag{3.43}$$

Since we know the values of evaluation points and also strength of magnetic field, we are (based on equation (3.37)) able to evaluate magnitude of magnetic dipole in these points. As figure shows, situation is symmetrical, which allows us to focus just on two of all five magnets – main magnet and slave one. For first estimation, we can say that

$$p_{M_j} = -\frac{p_{M_c}}{2}, \quad j = 1, 2, 3, 4. \tag{3.44}$$

Note that sign is the opposite of main magnet, because all four magnets have to complement with the main one, not repel. These data are all we need to know, enabling us to evaluate magnetic dipole moment of core magnet as

$$p_{M_c} = 16.3 \text{ A/m}^2. \tag{3.45}$$

Cross section of magnetic field strength in position $(0, y, 90)$ is shown in figure 3.5.

Producing moment described by equation (3.45) would require enormous current flow through coil made only by one loop, which is only an approximation of magnetic dipole. We have to keep in mind that actual magnetic field is produced by solenoids that consists
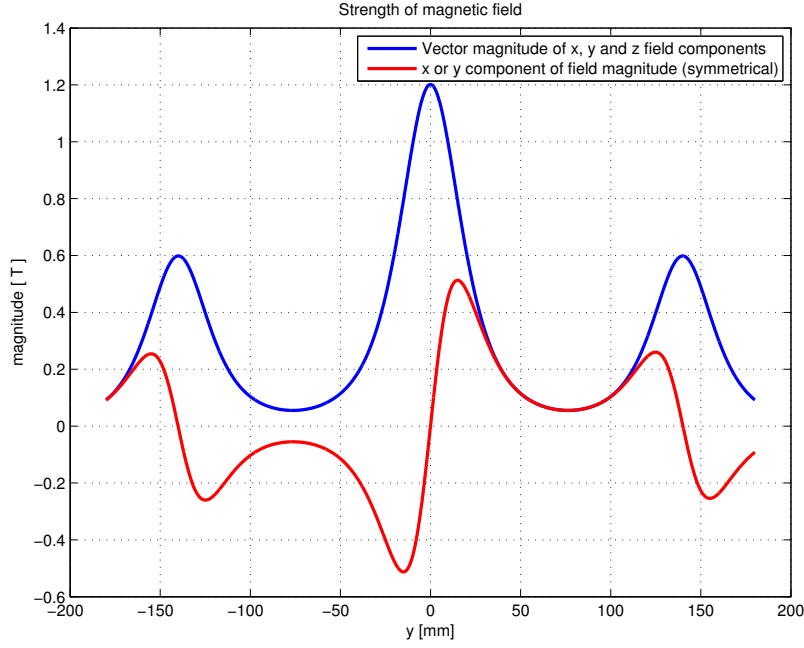
Figure 3.5: Cross section of magnetic field strength.

of hundreds of current loops, raising the possibility of creating strong and efficient magnetic fields just by applying few amperes of current. If we apply this setting to all slave dipoles, we get resulting magnetic field that surrounds the whole ion engine. Visualization of $x - z$ plane side section of Hall ion engine with magnetic field enabled and boundaries of discharge chamber is in figure 3.6. Top section is visualized in figure 3.7.
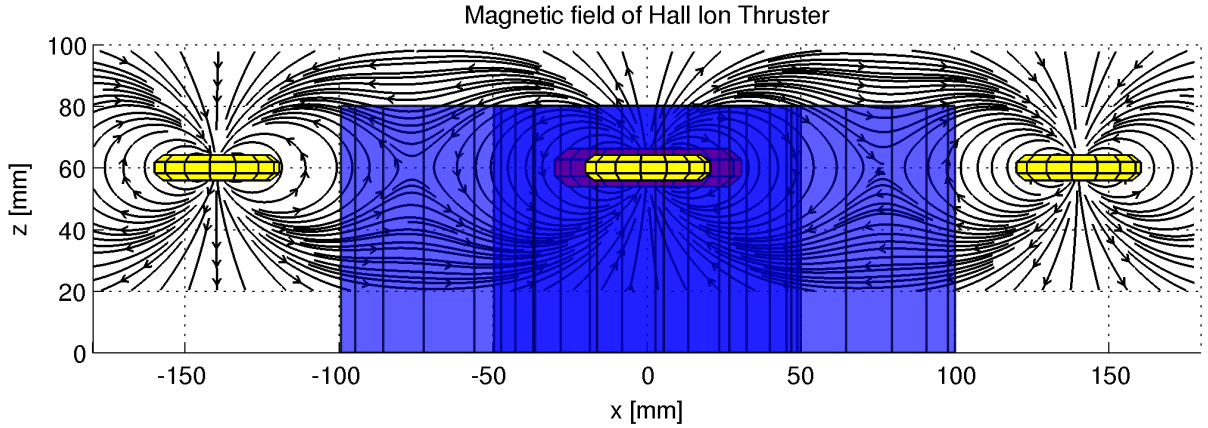

Figure 3.6: Side view of magnetic field of Hall ion thruster produced by 5 magnetic dipoles.

We can see that the behavior of magnetic field is as expected. From the side view we see that lines of magnetic inductance seal the discharge chamber, with most homogeneous shape just above and under the place of central line mentioned in figure 3.4. This is the part of field in which electron will be kept up steadily as it will experience highest magnitude of $\mathbf{E} \times \mathbf{B}$ drift. The most chaotic movement on the other hand can be expected at positions with heights equal to positions of magnetic dipoles, as field changes there dramatically, represented by slope with higher value of ∇B function.
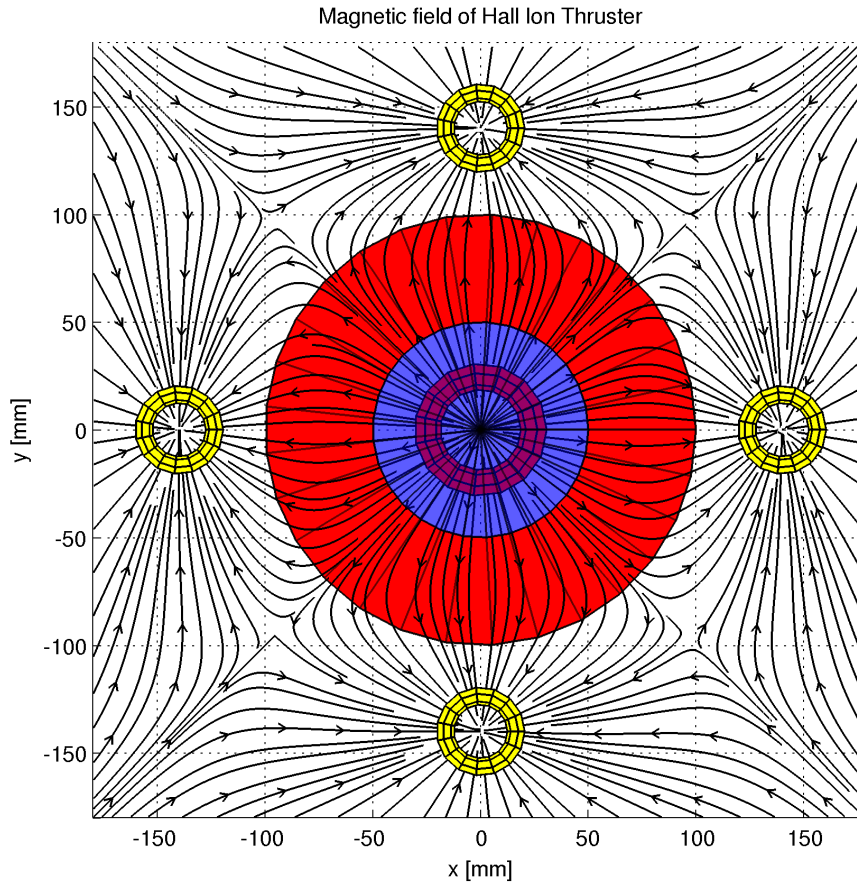
Figure 3.7: Top view of magnetic field of Hall ion thruster produced by 5 magnetic dipoles.

Top view reveals that slave dipoles are repelling each other, which is inevitable behavior due to same magnitude of magnetic dipole moment, which produces magnetic field of the same poles. This fact can be represented by a simple analogy of a child that put two solid magnets of the same poles together and feel that they do not like each other that way. Previously we talked about the possibility of increasing the number of slave magnets, to create more homogeneous and stable magnetic field. We can see that number of these magnets would be strictly limited, because at certain point their repulsion will create even more unstable field. This would have to be managed by more complicated design.

3.4   OVERALL DESIGN OF ION ENGINE

After we introduced both electric and magnetic fields with basic design of the engine, we can visualize final composition of the whole unit, with acting electric and magnetic field, enclosed by dimensions of discharge chamber. This visualization is in figure 3.8, where also protective cylinders of slave magnets were added, as they resemble physical coating of solenoid that would be added while constructing functioning version of this engine.
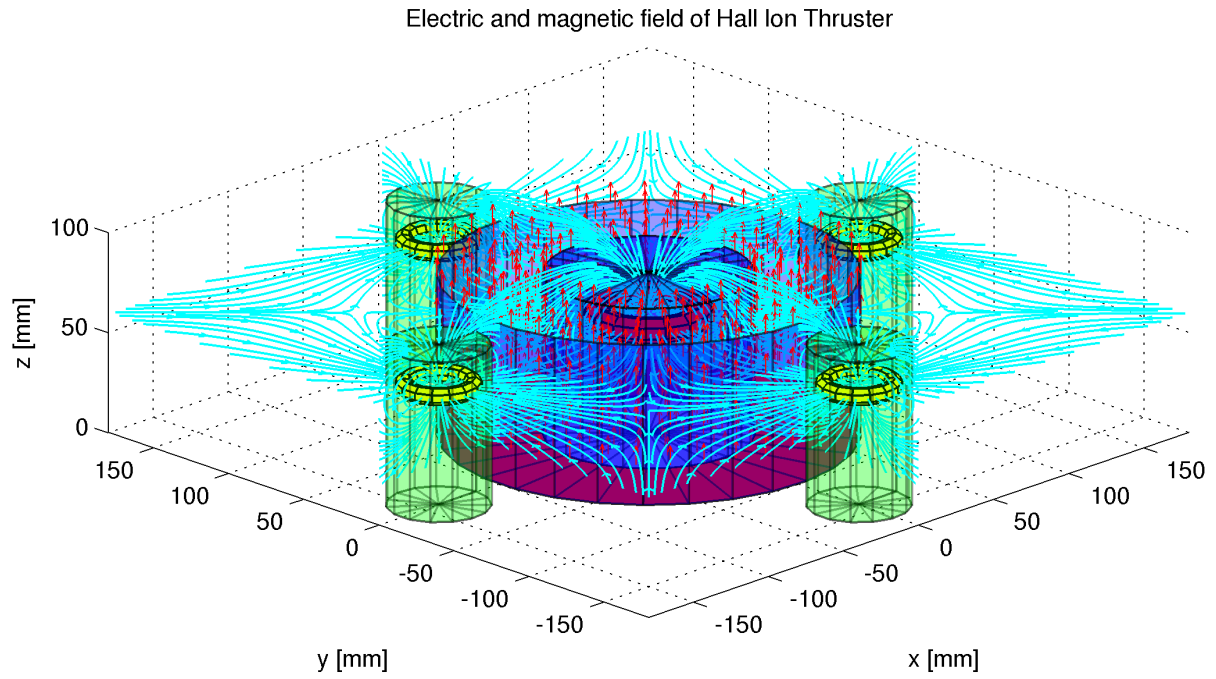
Electric and magnetic field of Hall Ion Thruster

Figure 3.8: Final composition of electric and magnetic fields of the engine.

CHAPTER 4
THEORETICAL INTRODUCTION FOR NUMERICAL SIMULATIONS

4.1 INTEGRATION METHOD

When discussing various electromagnetic configurations and simulating particle motion inside, we have to think of a proper method for these simulations. Several integration methods were developed, such as:

- Newton-Euler method
- Leap-Frog method
- Heun's method
- Runge-Kutta method
- Dormand-Prince method
- Boris-Buneman method

and the list goes on. The main difference is in the type of extrapolation, in other words – how is the next step determined. Every method listed uses different approach to solve this problem, where the least trustworthy is Newton-Euler method and the most trustworthy Runge–Kutta or Dormand-Prince method. These methods are universal and can be used not only in particle simulations, but also in much more, heavily different fields. In contrast, Boris–Buneman scheme is used mainly with numerical simulations of particle motion, however specific conditions must be applied to use this scheme. Dormand-Prince is also a well example of method that is based on other method's principle and modified. Algorithm is practically the same as in Runge–Kutta method, however Dormand-Prince uses more weighted averages and mid-point evaluations with addition to variable integration step. This allows it to reach 5-th degree of precision, whereas Runge-Kutta method is only 4-th degree, mostly with fixed integration step.

We will not include deeper explanation of this numerical schemes, however more information can be found in [8]. For illustration of how much of an impact can numerical method posses for the exactly same instance of problem being solved (in this case, particle in homogeneous electric and magnetic cross fields), two samples are shown in figures 4.1a and 4.1b.

In this thesis, numerical methods such as Dormand–Prince and Runge-Kutta were used. Dormand–Prince was applied through well–known MATLAB® *ode45* function. Runge–Kutta algorithm with fixed step for MATLAB® was written by myself and is available to anyone who do not hesitate to contact me.
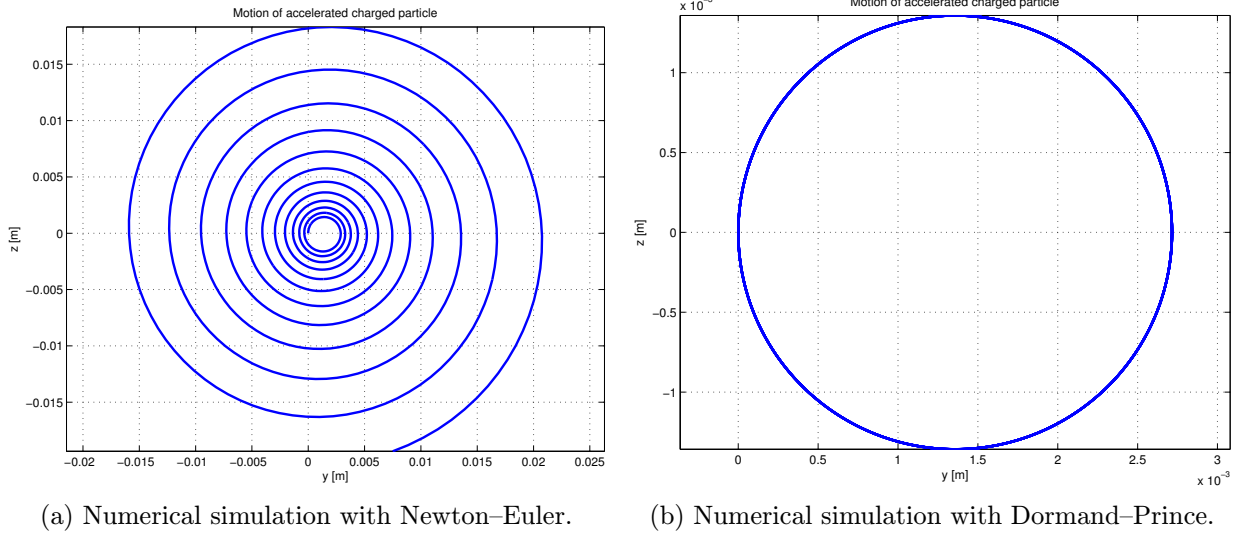
(a) Numerical simulation with Newton–Euler.

(b) Numerical simulation with Dormand–Prince.

Figure 4.1: Impact of various numerical methods.

4.2   DIMENSIONLESS EQUATIONS

Various simulation techniques were developed in past decade, relying on various techniques. The most widely used are direct simulations of any physical object or quantity behavior, for instance simulations of inverse pendulum and its regulation, most common in the theory of systems and control. These simulations works with direct physical dimensions of these objects, while extrapolating each step of their behavior. However, while discussing motion of elementary particles, this approach cannot be used, because doing so may lead to unreliable results. Reason is simple – mass and elementary charge of each particle. In computer science, such small numbers may cause overfloat, leading to fail results. Possible correction is modification of equations of motion to dimensionless equations, where all sizes are in unitary scales. This section will cover this problem.

4.2.1   EQUATIONS FOR ELECTRON MOVEMENT

Our equations of motion for electron movement, as described in equation (2.12), are:

$$m_{\mathrm{e}}\frac{d^2\mathbf{r}_{\mathrm{e}}}{dt^2} = -Q\mathbf{E} - Q\left(\frac{d\mathbf{r}_{\mathrm{e}}}{dt} \times \mathbf{B}\right). \tag{4.1}$$

We can now define our dimensionless equations through set of equations:

$$\mathbf{r}_{\mathrm{e}} = \bar{\mathbf{r}}_{\mathrm{e}}r_{\mathrm{e}_0}, \tag{4.2}$$

$$t = \bar{t}t_0, \tag{4.3}$$

$$\mathbf{E} = \bar{\mathbf{E}}E_0, \tag{4.4}$$

$$\mathbf{B} = \bar{\mathbf{B}}B_0, \tag{4.5}$$

$$m_{\mathrm{e}} = \bar{m}_{\mathrm{e}}m_{\mathrm{e}_0}, \tag{4.6}$$

$$Q = \bar{Q}Q_0, \tag{4.7}$$

where dashed variables are unitary and dimensionless, while variables with index 0 are their multiplications, producing original variable when combined. Substituting into equation (4.1) we get

$$\frac{m_{e_0} r_{e_0}}{t_0^2} \bar{m}_e \frac{d^2 \bar{\mathbf{r}}_e}{d\bar{t}^2} = -Q_0 E_0 \bar{Q} \bar{\mathbf{E}} - \frac{Q_0 r_{e_0} B_0}{t_0} \bar{Q} \left(\frac{d\bar{\mathbf{r}}_e}{d\bar{t}} \times \bar{\mathbf{B}} \right). \tag{4.8}$$

This result can be adjusted as

$$\bar{m}_e \frac{d^2 \bar{\mathbf{r}}_e}{d\bar{t}^2} = - \underbrace{\frac{Q_0 E_0 t_0^2}{m_{e_0} r_{e_0}}}_{=1} \bar{Q} \bar{\mathbf{E}} - \underbrace{\frac{Q_0 B_0 t_0}{m_{e_0}}}_{=1} \bar{Q} \left(\frac{d\bar{\mathbf{r}}_e}{d\bar{t}} \times \bar{\mathbf{B}} \right), \tag{4.9}$$

where we already underbraced primary conditions in order for equations to work properly. If we exclude time from one of the conditions and substitute it into another, we get the following set of equations:

$$\frac{E_0 m_{e_0}}{r_{e_0} Q_0 B_0^2} = 1, \tag{4.10}$$

$$\frac{Q_0 B_0 t_0}{m_{e_0}} = 1. \tag{4.11}$$

In the end, we have set of 6 unknown variables and two equations, which means we have to choose four variables with two odd variables dependent on previous four. In our case, the choice is simple, since we know mass of electron, its charge and central line of discharge chamber. Nominal magnetic field B_0 can be chose by its real value, therefore making it unitary. Remaining variables can be computed by conditions given.

4.2.2 EQUATIONS FOR ION MOVEMENT

Equations for ions are derived by the same principle, where the final output is

$$\bar{m}_i \frac{d^2 \bar{\mathbf{r}}_i}{d\bar{t}^2} = \bar{Q} \bar{\mathbf{E}} + \bar{Q} \left(\frac{d\bar{\mathbf{r}}_i}{d\bar{t}} \times \bar{\mathbf{B}} \right), \tag{4.12}$$

with conditions

$$\frac{E_0 m_{i_0}}{r_{i_0} Q_0 B_0^2} = 1, \tag{4.13}$$

$$\frac{Q_0 B_0 t_0}{m_{i_0}} = 1. \tag{4.14}$$

All of these variables were included in numerical schemes used to compute simulations, however with unitary values, making no difference to the output produced whatsoever, since they were not currently needed. This technique is prepared to use in future research.

CHAPTER 5
NUMERICAL SIMULATIONS

In this chapter, we will be finally discussing probably the most interesting part of this thesis, which are simulations of particles in ion engine. All of the simulations were made with magnetic field set to nominal value of 0.0554 T in position $\mathbf{r}_{\mathrm{B}_0}$.

5.1 ELECTRON MOVEMENT IN HALL EFFECT THRUSTER

5.1.1 INITIAL CONDITIONS

There are very specific initial conditions for electrons, since they are being emitted from hot electrode or multiple of electrodes (mostly two) right above the edge of discharge chamber, with position vector of

$$\mathbf{r}_{\mathrm{elctr}} = (80, 80, 90) \text{ mm.} \tag{5.1}$$

Kinetic energy of molecule is roughly equal to temperature of such electrode, as it approximates internal energy of gas composed of one molecule – in our case, xenon. Internal energy of one electron with 3 degrees of freedom emitted from electrode is thereabouts

$$\mathcal{U} \approx \frac{3}{2} k T_{\mathrm{emp}}, \tag{5.2}$$

where T_{emp} is temperature in Kelvin and k is *Boltzmann constant*. Various electrodes exist, whereas we can assume the case with electrode glowing at temperature 5000 K. For such temperature, energy of electron, created by this electrode, is approximately

$$\mathcal{U} \approx 1.0355 \times 10^{-19} \text{ J,} \tag{5.3}$$

which correspond to 0.6463 times energy of one eV (electronvolt). From definition of kinetic energy for electron, we are able to approximate initial condition of velocity of electron, which is

$$\|\mathbf{v}_{\mathrm{e}_0}\| \approx 4.7681 \times 10^5. \tag{5.4}$$

This initial condition may seem large enough, yet it is almost completely ignored and magnetic field plays with the electron in the way it wants, not looking at initial conditions whatsoever. Reason for this behavior was previously spoken many times – mass of electron. This mass and also charge of electron is so negligibly small, it does not stand a smallest chance compared to electric field created by potential of 1000 V or substantial

magnetic field of around 0.05 T. For integrity of all physical conditions, we are still presenting this calculation.

From now on, if initial velocity of electron would be crucial, it will be presented in description of particular simulation. If no conditions of velocity are presented, reader may think of any value reading from 0 m/s to 500 000 m/s.

5.1.2 MOTION OF ELECTRON IN MAGNETIC DIPOLE

Although this scenario does not resemble anything in real world situation, it is perfect, yet purely theoretical example of how magnetic field is interacting with moving particles – electrons.

First of all we have to define few key characteristics. Layout of engine dipoles is the same as in figure 3.8, however without the electric field, as shown in figure 5.1.
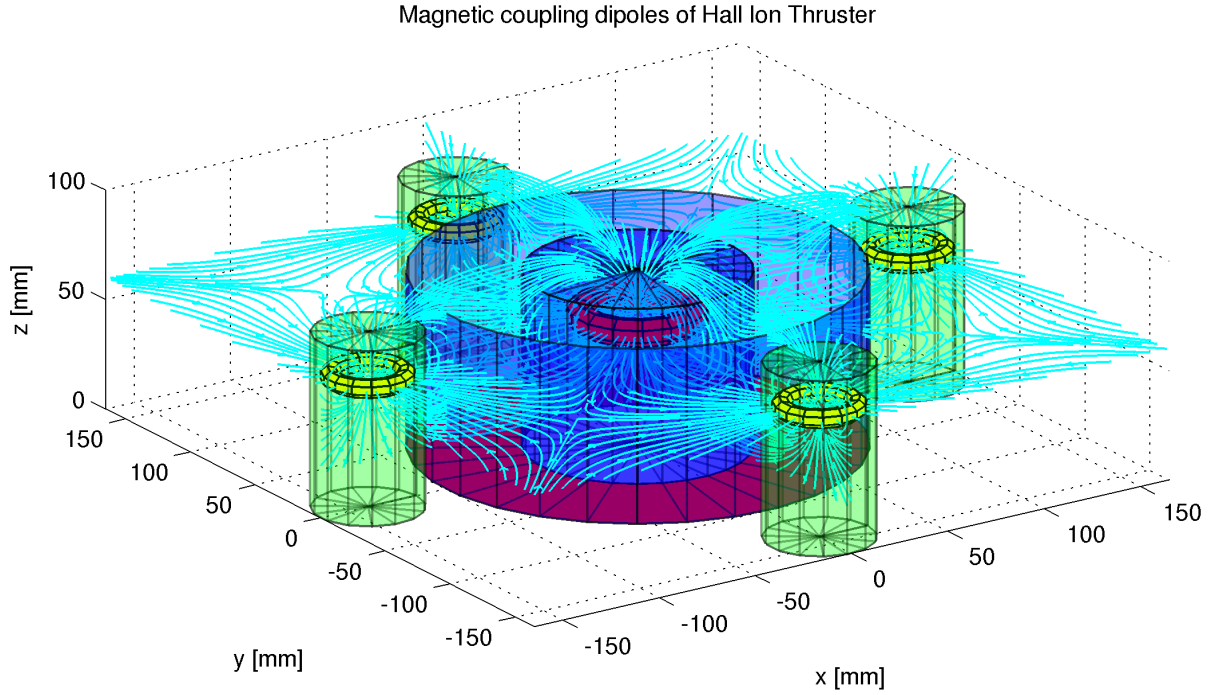
Figure 5.1: Magnetic dipoles enclosing discharge chamber.

For demonstration principles, initial velocity is

$$\|\mathbf{v}_e\| = 2 \times 10^6 \text{ m/s,} \tag{5.5}$$

which corresponds with energy of

$$\mathcal{T}_e = 11.373 \text{ eV,} \tag{5.6}$$

and simulation time of $t = 122.2 \ \mu$s. Initial placement is in vector $\mathbf{r}_{\text{elctr}}$ previously defined, which resembles nozzle of electrode. Simulation is shown in figure 5.2.
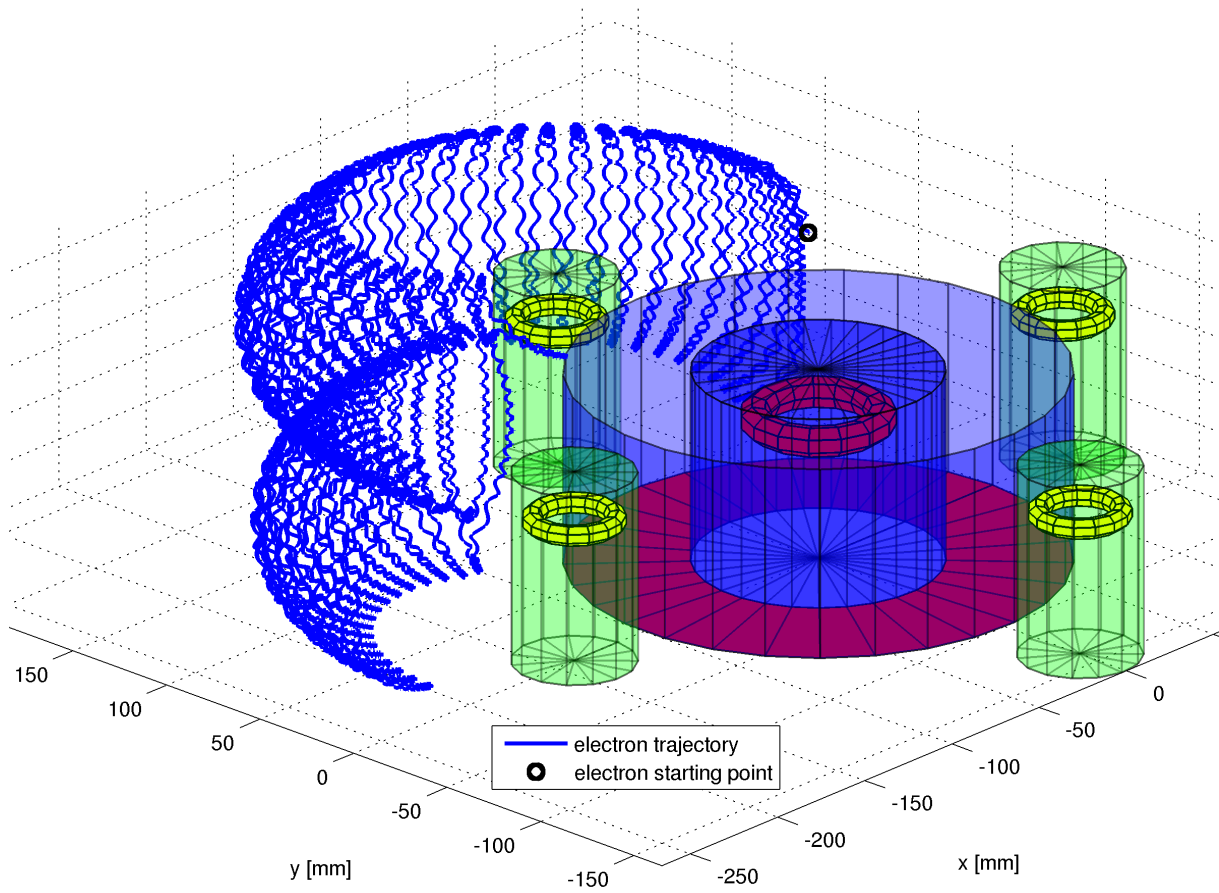
Figure 5.2: Magnetic dipoles enclosing discharge chamber.

As we can see from simulation, each electron will be in next simulations experiencing much more difficult motion than just pure $\mathbf{E} \times \mathbf{B}$ drift. For instance, present is drift caused by centripetal force or drift caused by $\boldsymbol{\nabla} B$. Electron gyrates around discharge chamber in a slightly more complex pattern, reflected by magnetic mirror. Another gyrating motion is around radial field lines of vector field $\mathbf{B}$. Also, as seen from simulation time, azimuthal drift has extremely slow velocity.

The result itself is not that useful for any computation regarding thrust or function of ion engine, it is however rather beautiful example of what electron motion actually consists of. After applying axial electric field, behavior shown is no longer seen, where rather gyration around the chamber is the main observed effect. In tiny pieces of movement, however, small fragments prevail and are indeed recognizable. We will refer to those details in upcoming simulations, where sometimes, they may cause complete loss of balance and force electrons to move extremely chaotically, resulting in loss of electrons and lowered engine efficiency, since such electrons will hit the walls of discharge chamber, complete the circuit by connection with anode and cease to exist.

Interesting in this case is plot of velocity, more specific tangential velocity – magnitude of velocity vector. As shown in figure 5.3, we see one extremely important fact about the whole magnetic field, which is consisting of core ans another four slave magnetic dipoles.

This field does not increase, nor decrease the energy of electron, rather just plays with the one that was given to it. This is highly important factor, since we know that magnetic field was, indeed, constructed in the proper way.
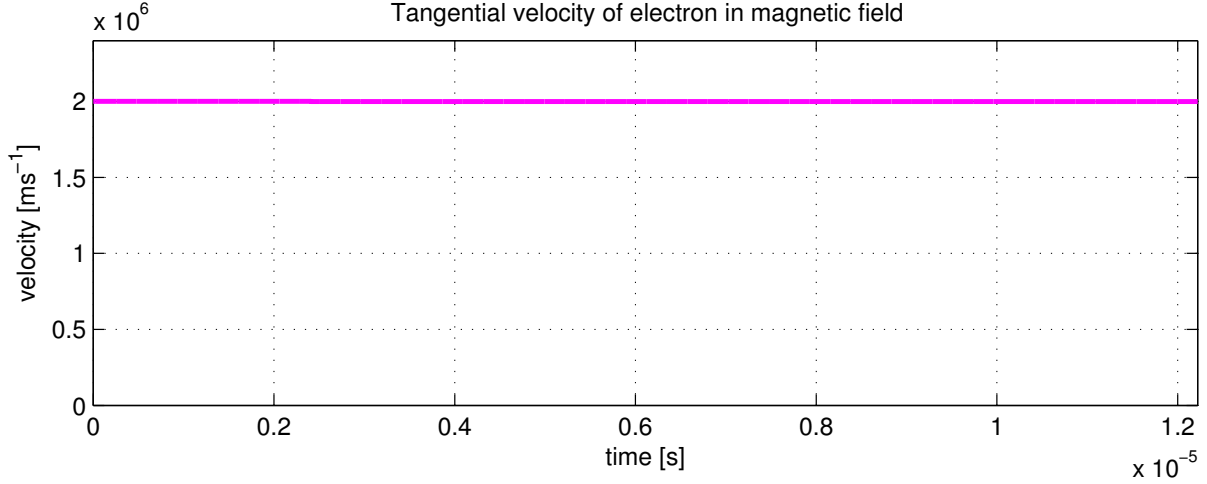

Figure 5.3: Tangential velocity of electron stays on the same level.

We will move further, however more theory about exactly this problems are discussed in [8].

5.1.3 MOTION OF ELECTRON IN AXIAL ELECTRIC AND RADIAL MAGNETIC FIELDS

We now continue by properly adding axial electric field shown in figure 3.3 with final look as shown in 3.8. All of the characteristic field properties were designed in chapter 3, which means we can move directly to simulations.

We can think of several initial placements. One in position where electron is leaving nozzle of electrode. Another in position where magnetic field was defined as nominal, which may (with light deviations) resemble initial conditions that occurs while gas of xenon is ionized, thus releasing additional electrons. At last, we can think of position where magnetic field vary too much, leaving us with abandonment of adiabatic approximation.

First of all, let us focus on initial condition based on placement where nozzle of electrode may be, with vector of

$$\mathbf{r}_{e_{\text{init}}} = (80, 80, 90) \text{ mm.} \tag{5.7}$$

Simulation in this placement is shown in figure 5.4 and 5.5.

As we can see, behavior of electron has changed radically, truly gyrating around discharge chamber in a circular manner. We are even able to see the pattern of gyration, which is secondary product of geometric layout we designed. This pattern can be greatly normalized and stabilized by increasing number of slave magnetic dipoles, which will distribute magnetic field more steadily around discharge chamber. Optimal configuration
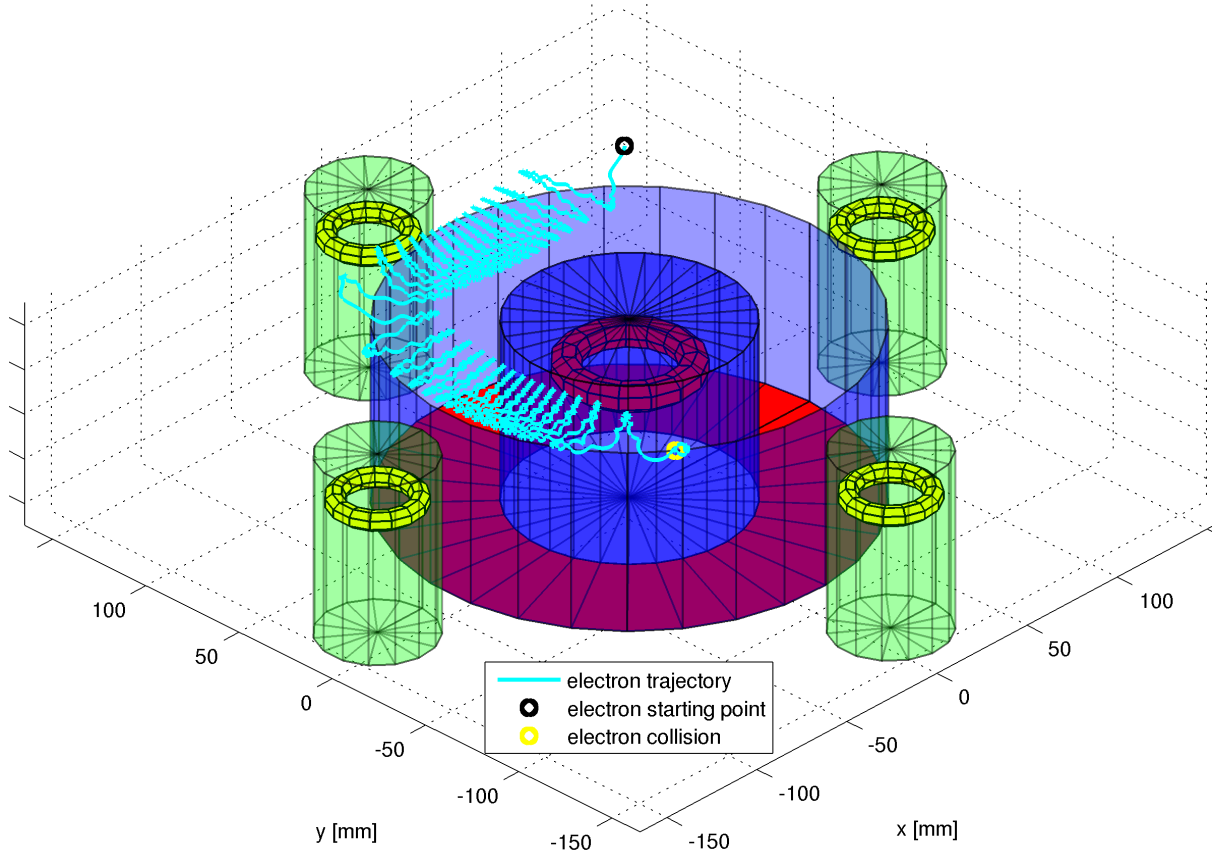
Figure 5.4: Simulation of electron in presence of electromagnetic field.

now shows up to be 8 magnetic dipoles, represented by solenoids in real world scenario.

Another magnificent object we should be curious about is the yellow dot, representing, place where electron reached (theoretically) boundary of discharge chamber, yielding to collision. In real world application, electron would loose all of its energy. Two possibilities exists. It would disappear inside the molecular structure of material walls of chamber are made of, or began to fall down to anode. If electron would survive the collision, it will regain energy thanks to electric field, followed by repeated capture by magnetic field, since electron was located at the top of discharge chamber and not the bottom, where possibility of electron to diversify from magnetic field is much more plausible. In case of computer simulation, equations of motion were dynamically modified to watch for mathematical description of discharge chamber boundary, yielding to stop of simulation if located nearby.

Interesting part to watch is also result for tangential velocity, which is shown in figure 5.6, where increase of electron's energy is product of electric field acting on it.

We can see that velocity gain is indeed extreme. This is due to strong potential of 1000 V provided by anode, which is like a standing giant for our poor electron. Relativistic equations we derived previously were used, even that relativity does not account on
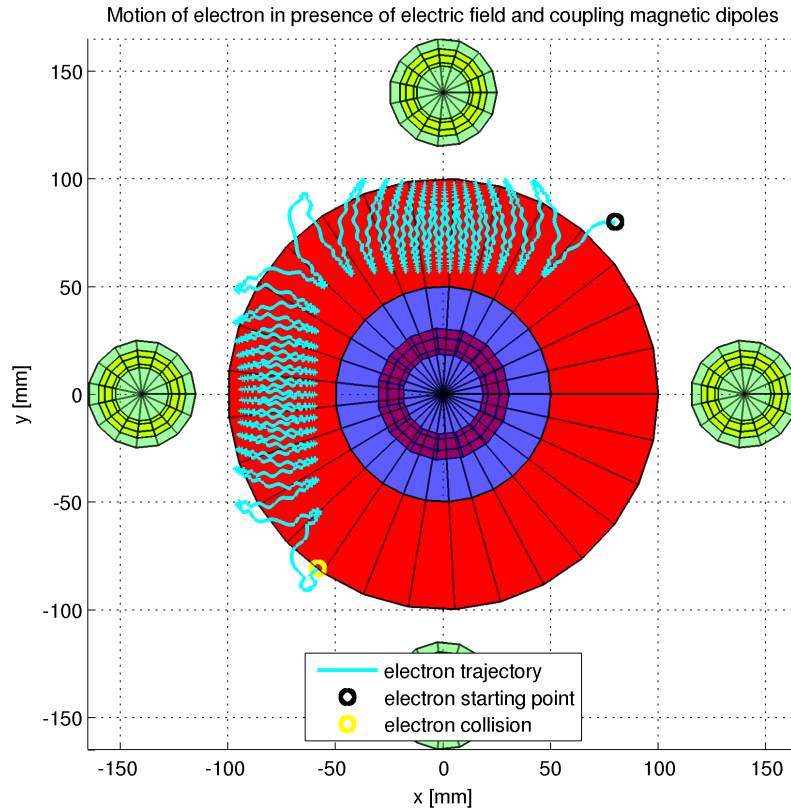
Figure 5.5: Simulation of electron in presence of electromagnetic field.
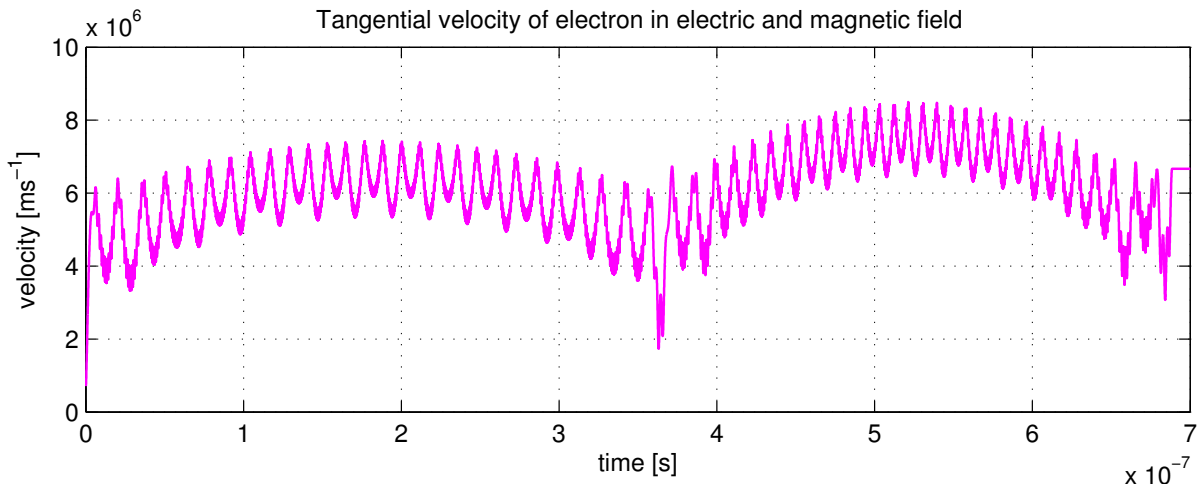

Figure 5.6: Tangential velocity of electron located in axial electric and radial magnetic field.

this level significantly. Time base of this simulation was 0.7 μs. Electron hit surface of discharge chamber few ns earlier.

Let us now think of another initial electron placement – inside the chamber. This may happen particularly when atoms of xenon are ionized, detaching another electron. Simulation results for three electrons spanned across x axis are in figure 5.7, where the most

stable is located with condition

$$\mathbf{r}_{e_{init}} = (76, 0, 60) \text{ mm}, \tag{5.8}$$

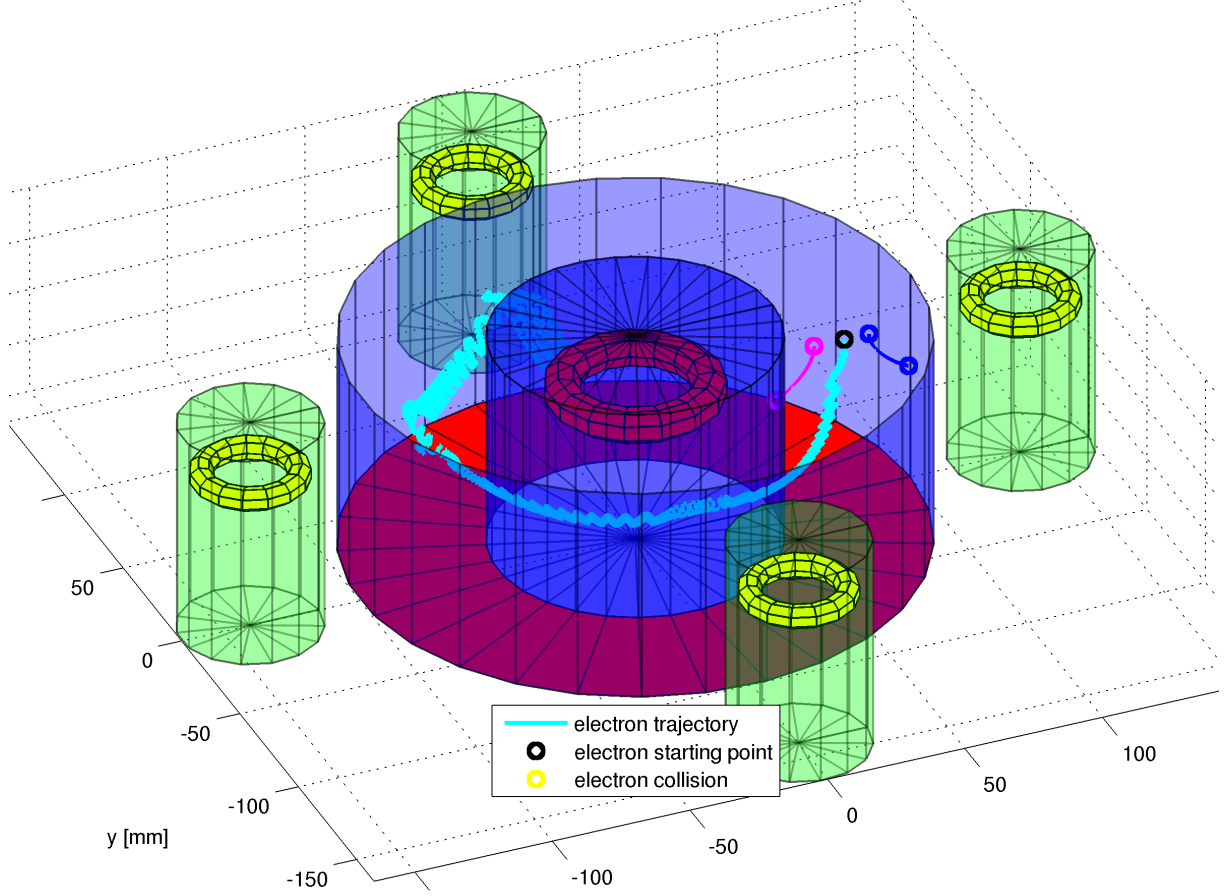therefore located at the height of magnetic dipoles.

Figure 5.7: Simulation of electron in presence of electromagnetic field.

We can see that millions of different electrons with millions of various conditions can behave much more differently. The most stable electron in this simulation is just few millimeters away from his two neighbors, which were pulled by core and slave magnet respectively, depending on which of the magnets were closer. Fascinating behavior in this simulation is represented by electron moving around the first slave dipole, seen by electron as third. Detail of this simulation is in figure 5.8.

Figure 5.8 is truly stunning, where I found myself watching on the result for few minutes rigidly. Fans of *Alien* franchise may shed a tear, since result is heavily similar to *facehugger* from these movies. Therefore from now on, likewise shapes are defined by this description as facehuggers.

We can see that electron motion around this particular path representing our facehugger is largely complex, with no possibility of analytical derivation whatsoever. Various connections of motions and drifts are present, for instance rotation around lines of magnetic field, $\mathbf{\nabla} B$ drift and mainly $\mathbf{E} \times \mathbf{B}$ drift. Time base for this simulation was 1 μs.

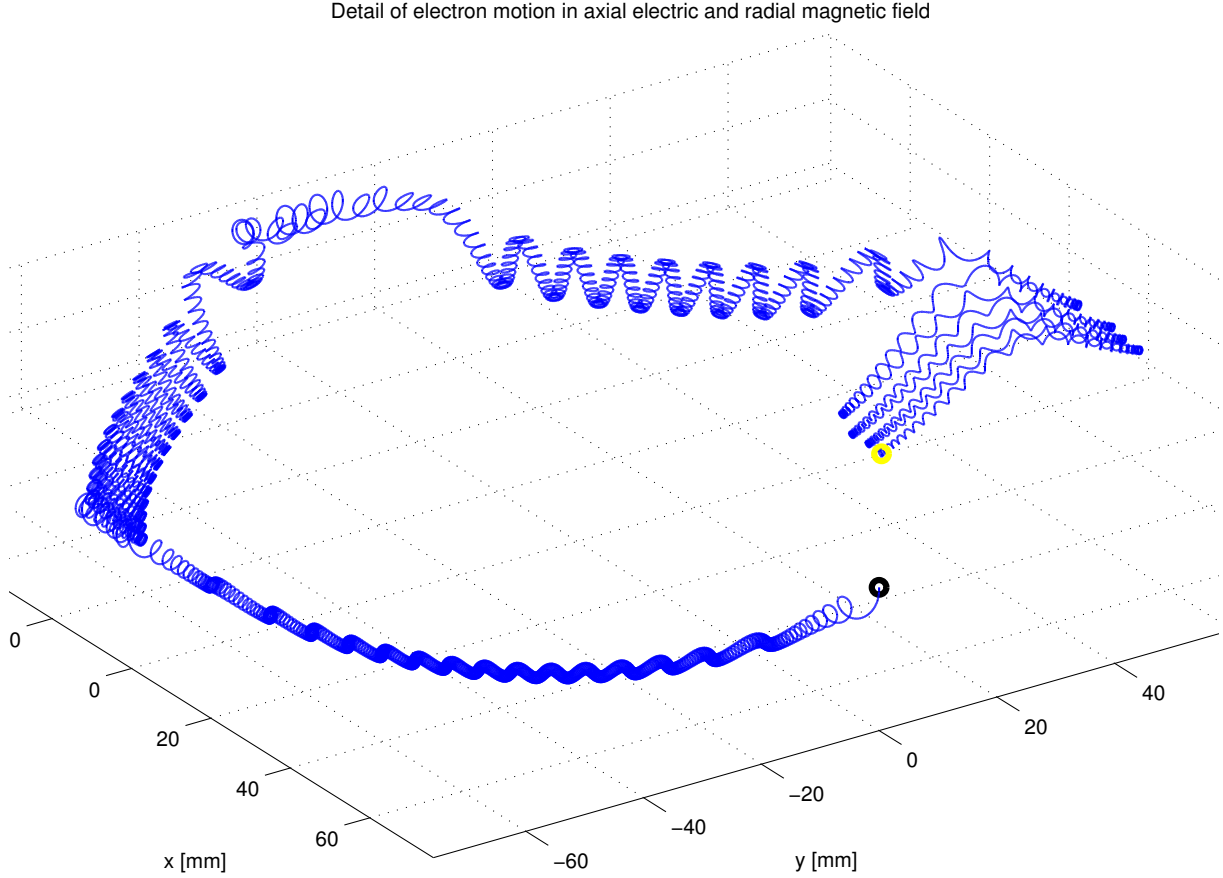Detail of electron motion in axial electric and radial magnetic field

Figure 5.8: Detail of facehugger.

5.2 ION MOVEMENT IN HALL EFFECT THRUSTER

Compared to electron movement, ions are generally boring. However they are the main part of spacecraft's acceleration, therefore the most important part of this thesis.

As discussed earlier in chapter 3, ions feel different potential than electrons, since electrons are carriers of charge. This is of course only an approximation because electrons repel each other, however we do not consider mutual interaction between particles.

Compared to electrons, trajectory of ions can be derived analytically, or at least very closely approximated, since ions do posses one interesting thing in their behavior, which will be explained shortly.

We know that height of discharge chamber is 80 mm and that force that ions feel is mostly

$$m_i\ddot{\mathbf{r}}_i = Q\mathbf{E}. \tag{5.9}$$

This is all we need to know to directly integrate this equation, producing analytical equations for position and velocity as

$$\mathbf{r}_\mathrm{i} = \frac{Q}{2m_\mathrm{i}}\mathbf{E}t^2, \tag{5.10}$$

$$\mathbf{v}_\mathrm{i} = \frac{Q}{m_\mathrm{i}}\mathbf{E}t. \tag{5.11}$$

We can compute time needed for ion to travel 80 millimeters on the top of discharge chamber, where this time is 3.8230×10^{-6} s. This result shows that while ion simply travels 80 millimeters, single electron may already be done gyrating roughly one thousand times around the discharge chamber. Simulation where this behavior is showed by fraction of that time for gyrating electron and accompanied ion is shown in figure 5.9.
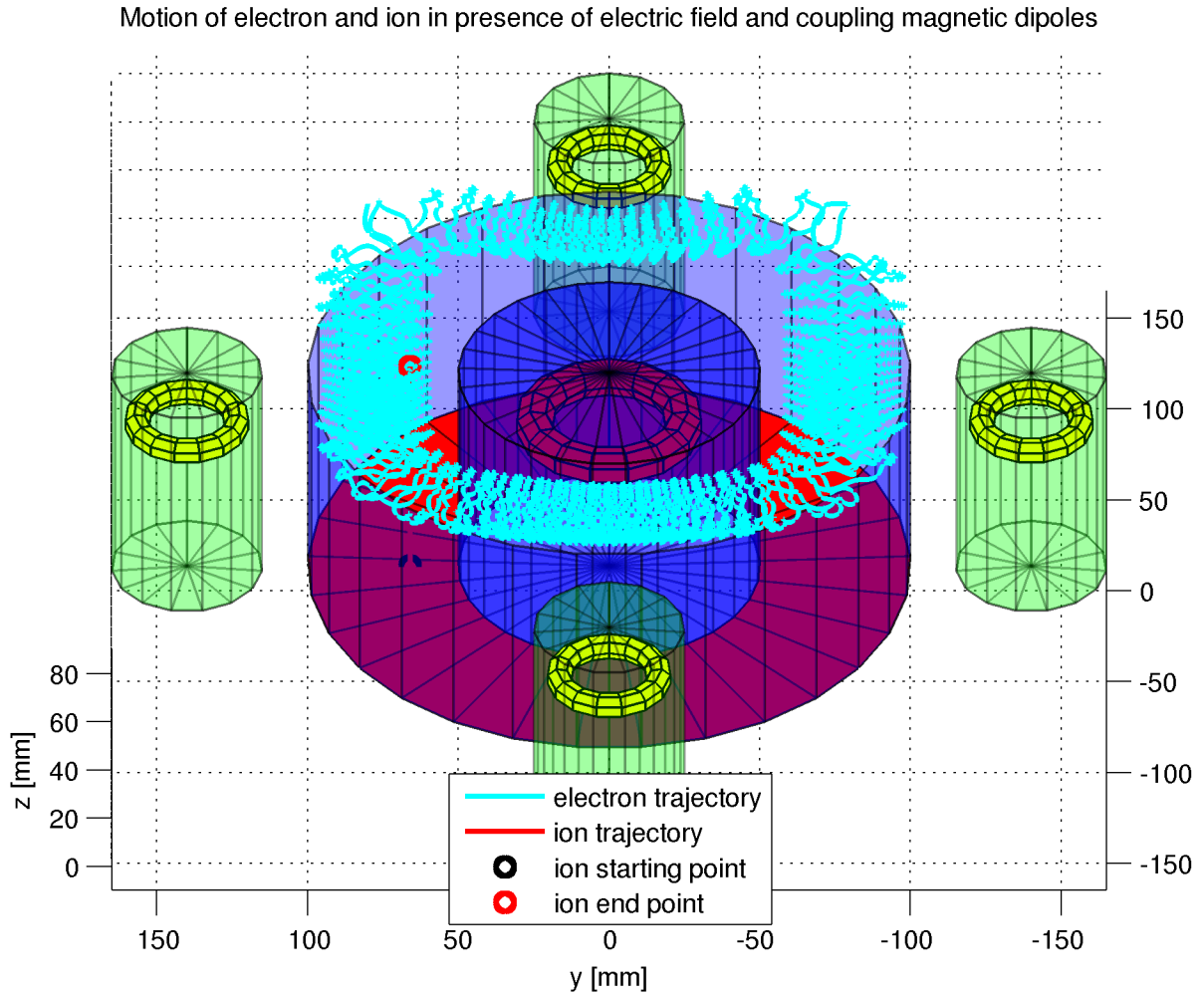

Figure 5.9: Multiple rotations by electron while accompanied by ion.

Initial condition for electron were used the same as in the first simulation for electrons, only difference that now with zero initial velocity, therefore causing no disturbances. Initial position of ion is

$$\mathbf{r}_{\mathrm{i_{init}}} = (0, 66, 0) \text{ mm.} \tag{5.12}$$

Detail of electron and ion motion in axial electric and radial magnetic field
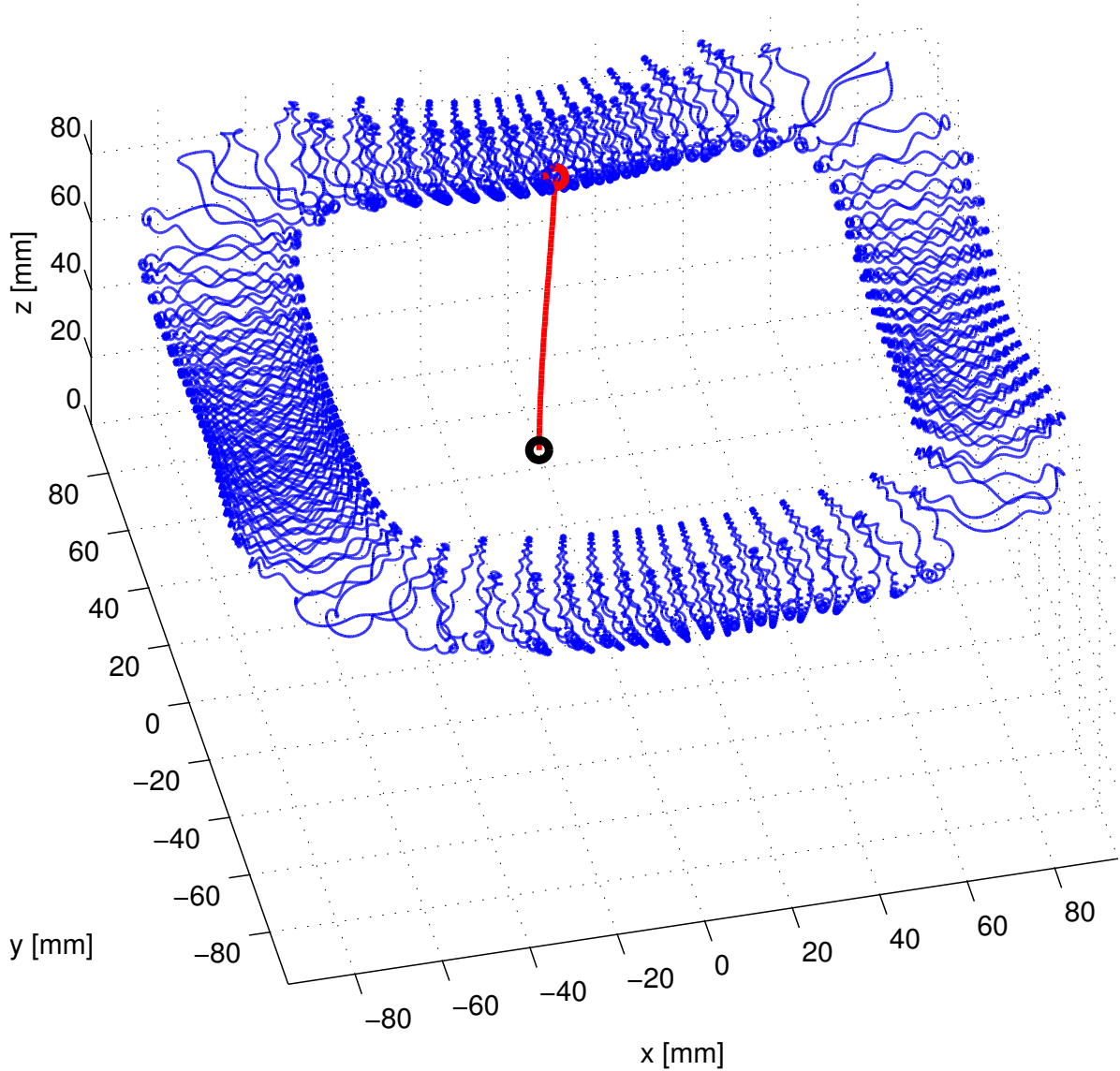

Figure 5.10: Multiple rotations by electron while accompanied by ion.

Detail of this simulation is in figure 5.10.

We previously told that ions posses one interesting property, which can be seen on previous figure. Ions are slightly shifted. There is no other reason for this behavior than magnetic field. Just now we are able to see the contrast between ion and electron and imagine how negligible electron actually is. This ion shift however reduces thrust produced by engine, because it removes portion of force that is being transfered, reducing only to formula defined in equation (2.28). Simulation showing rotation of ions are in figures 5.11 and 5.12.

This shift can be reduced or increased by changing the strength of magnetic field. This diverging field is widely know in ion engine propulsion systems, whereas effort is made
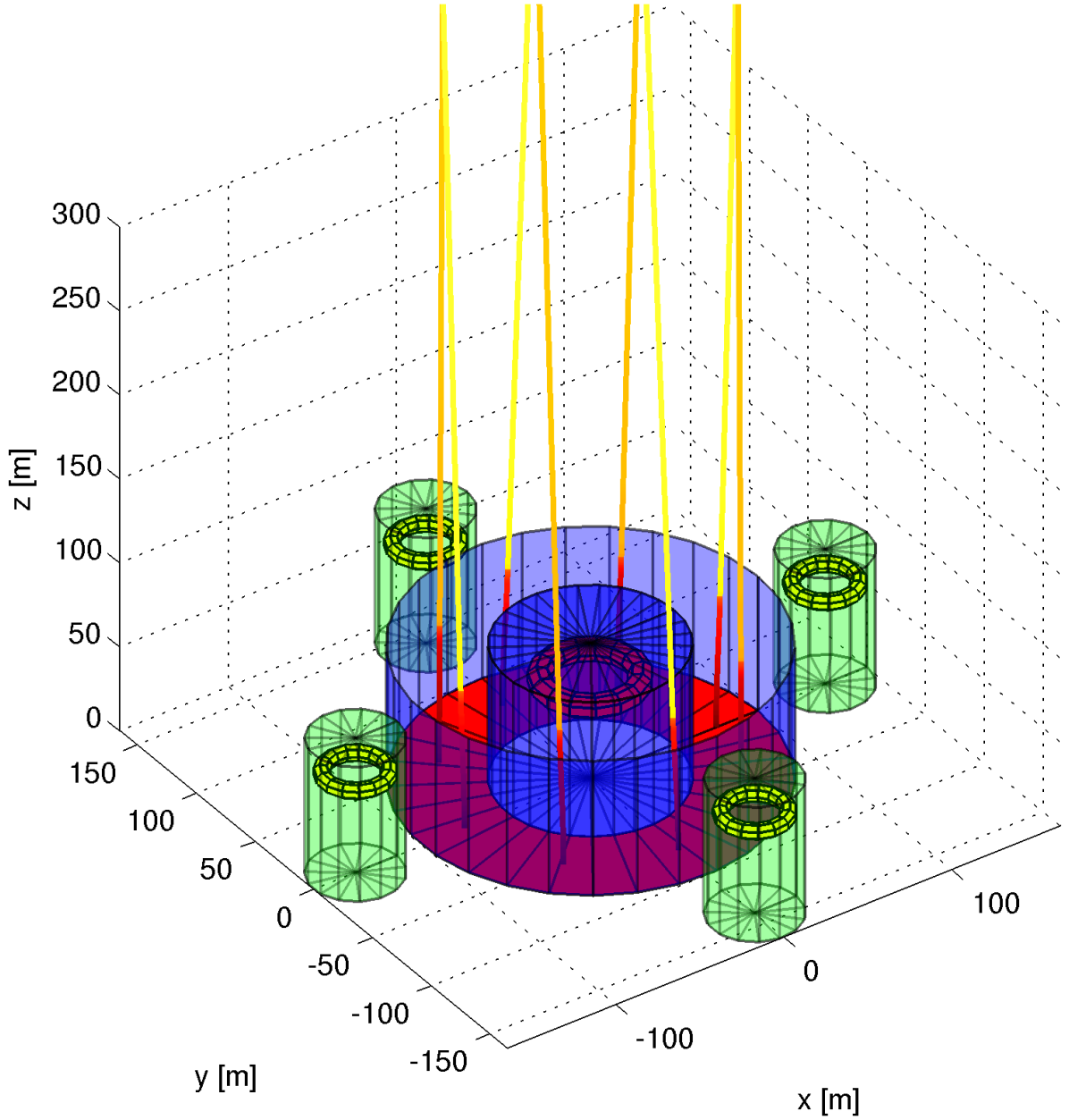
Figure 5.11: Rotation of ions due to magnetic field.

to develop such techniques that this (so called *plume*) of ions do not diverge, but also effectivity of engine remains the same. Top view in figure 5.12 shows how much can ions diverge.

Important factor for us is velocity of ions after leaving discharge chamber. This is shown in figure 5.13.

We can see that velocity raises constantly, which fits perfectly with analytical equation (5.11). Equations for simulations were dynamically edited in a way that allows ions to
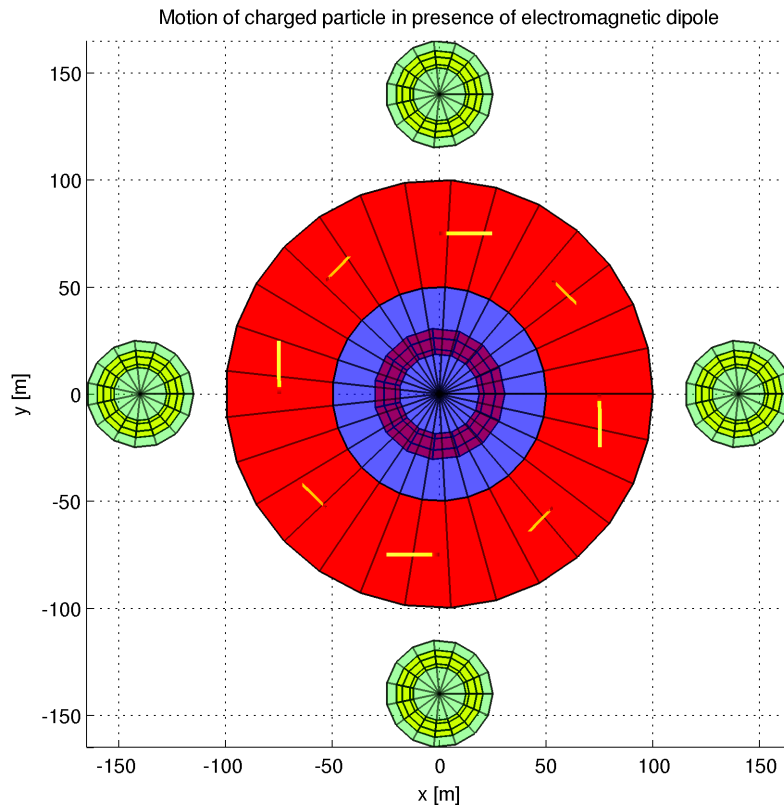
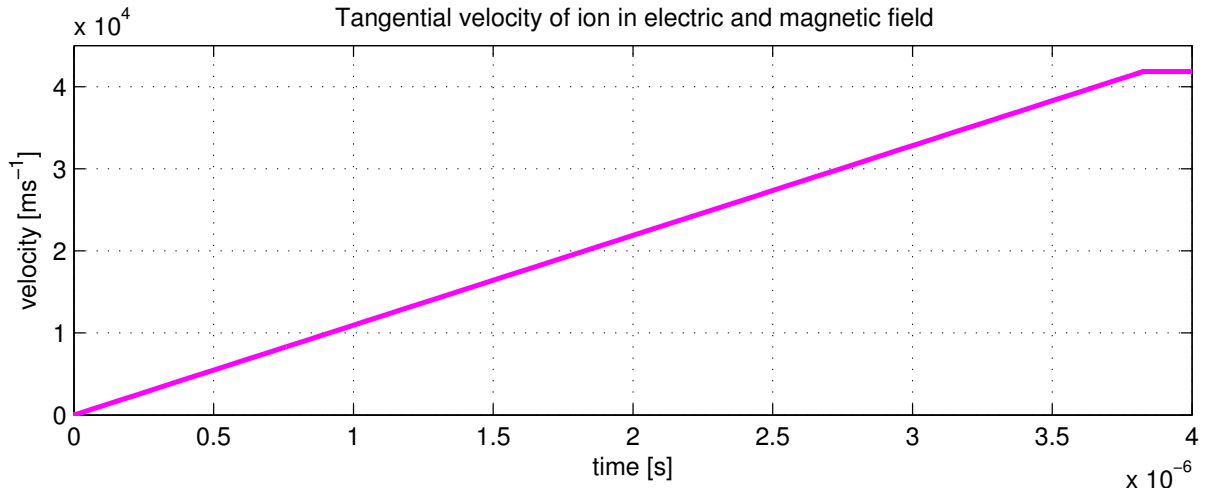Figure 5.12: Clockwise rotation of ions due to magnetic field – top view.

Figure 5.13: Velocity acquisition of ion while being accelerated in discharge chamber.

stop feeling potential difference after leaking to outer space. Equations then resemble the fact that ions are neutralized after leaving engine, with addition to rapidly decreasing electrical field, which is no longer constant as between anode and virtual cathode of discharge chamber.

In our simulation, exhaust velocity of leaking ion achieves magnitude of 41 852 m/s. Figure showing thrust acting on single ion is in figure 5.14.
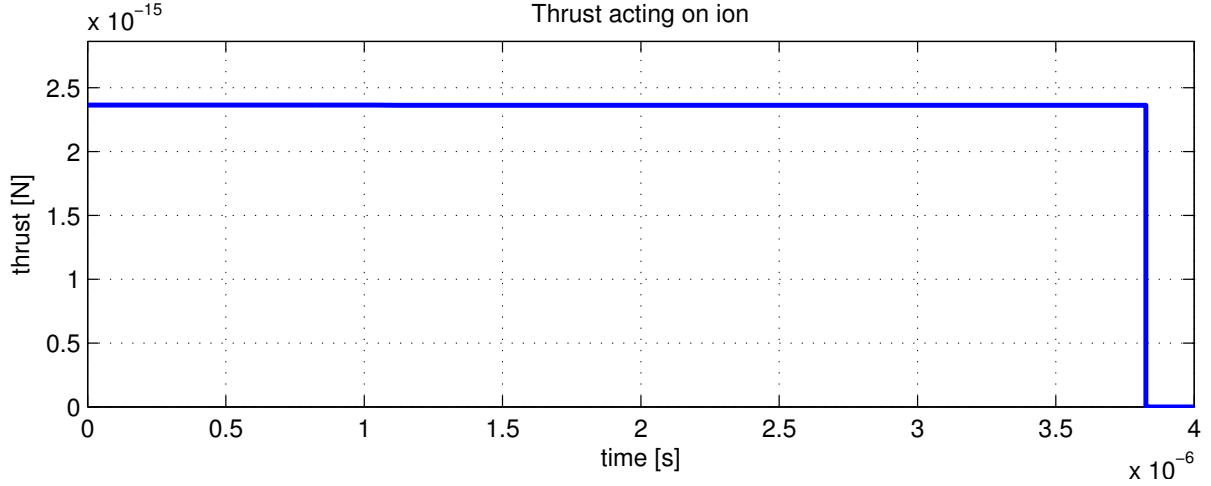
Figure 5.14: Force acting on single ion while being accelerated inside discharge chamber.

We can see that trust is being constant for the whole time, which resembles Lorentz force equation with its parameter $Q\mathbf{E}$. After ion leaves discharge chamber, thrust rapidly falls to zero. This behavior would be more smooth in real conditions, mostly because of ion neutralization, which doesn't happen exactly on the edge between inner space of discharge chamber and outer space. Force acting on a single ion can be written as

$$[\mathbf{F}_i]_z = \|\mathbf{F}_i\| \sin(\theta) = 2.3632 \times 10^{-15} \text{ N}. \tag{5.13}$$

All done in annular chamber high merely 80 millimeters.

5.3   THRUST GENERATED

With use of hypothetical derivation that were done in chapter 2, we are now able to compute theoretical thrust generation of our designed Hall effect ion thruster. For recapitulation, thrust produced by single ion is

$$[\mathbf{T}_i]_z = \|\mathbf{T}_i\| \sin(\theta) = \| - \mathbf{F}_i\| \sin(\theta) = 2.3632 \times 10^{-15} \text{ N}. \tag{5.14}$$

If we return to the part where we were discussing how many electrons could detach from 130 g of xenon, we come back with a value equal to Avogadro number N_A. If we substitute this number as number of ions N_i and use equation (2.29), we can compute final thrust generated by 130 g of ions. However, this value would resemble 130 g of xenon that are being accelerated instantly, which is not possible.

Unfortunately, being able to compute actual thrust generated by engine in active state would mean to define flow of propellant $\dot{m}_{ppl}$, which is an unknown variable, depending on various factors as pressure of gas, mechanical properties of anode that also serves as propellant distributor and more. Anyway, what we can compute is theoretical value of delta-v – velocity gain by certain amount of propellant, as derived in equation (2.46).

If we go back to introduction, we can read about space probe SMART-1, that hit the

surface of Moon on 3rd of September 2006. Mass of this probe at start was 367 kilograms, including propellant, which was nearly 80 kilograms of xenon gas. Well, let us suppose that mass of this propellant was our 130 grams. From simulations we know that exhaust velocity of ion is

$$v_{\text{ex}} = 41852 \text{ m/s}. \tag{5.15}$$

Let mass of our probe be

$$m = 367 - 80 + 0.13 = 287.13 \text{ kg}. \tag{5.16}$$

After using equation (2.46), we get that only 130 g of xenon, producing thrust through our theoretical hall effect ion thruster would increase velocity of probe by amount

$$\Delta v = 18.9531 \text{ m/s}. \tag{5.17}$$

That is an outstanding outcome of this thesis.

CHAPTER 6
CONCLUSION

As described in abstract and introduction, main aspect of this work was study of charged particle motion in Hall effect thruster, specifically stationary plasma thruster (SPT).

In theoretical part of the work, formulas were derived to support all of our efforts to characterize this type of thruster and behavior of particles located inside of electric and magnetic field produced by this thruster. For simulation of particle motion, relativistic differential equations were used, even despite the fact that output velocities of ion thrusters were known to be around 40 km/s. However for electrons, situation is different, since simulation results showed that velocity achieved of every electron can be greater than 10^6 or 10^7 m/s, which was later after consideration of all acting factors proved to be their most possible behavior. Even that most of the results with velocity values of 10^6 m/s and with relativistic approach don't generate observable changes compared to calculation with non-relativistic case, some of the results were in order of 10^7, which did produce small changes. Relativistic approach was beneficial here.

In order to characterize proper behavior of particles, specific electric and magnetic field was designed. Electric field was approximated as electric field of charged plate. This approximation is not the closest possible approximation we could get and even that it is actually more than satisfactory, more complex definition of this field would produce more accurate results. However, greater impact than geometrical representation, possibly greatest of all, is number of electrons gyrating on boundary of discharge chamber. For our simulations, we selected nominal value of electrons to be 10^{10}, with potential generation roughly -180 V. This number is however highly speculative, since in time of writing this thesis, not enough data were available to found out what is the proper number. Increase of electron quantity only by one thousand times would produce potential of -180 kV, which is extremely high value, possibly unrealistic. While designing this virtual cathode, another speculation was made, and that is the fact that electrons feel different electric field than ions, since ions are located between anode and virtual cathode, feeling two different energy sources, while electrons feel only potential of anode. This approximation takes account only on low levels, that is also reason why potential of -180 V was selected. More faithful characteristic of electric field, solving this problem, would mean to include interaction between all particles, which would be electron – electron, ion – ion and electron – ion. Such characterization will greatly affect all of the results, making them more accurate. Also, moving particles creates their own magnetic field, interacting with magnetic field of thruster and other particles, making it much more difficult problem,

as it is no longer question of electric potential only, but also electromagnetic interaction generally. This is far beyond the problems discussed in this thesis.

Magnetic field was created by combination of 5 magnetic dipoles, where core dipole is located inside discharge chamber and four slave dipoles are located around the core, 90 degrees azimuthally. Strength of magnetic field was defined for quasi-potential well, that is shown in figure 3.5, where behavior of particles is the most stable, as magnetic field geometrically changes at the lowest level. Strength of this field was set to 0.0554 T with producing magnetic dipole moment of 16.3 $A \cdot m^2$. Characterization by magnetic dipoles is also only an approximation, but on far lower level than not including interaction between particles. More accurate magnetic field would be produced by solenoids, which are actually just magnetic dipoles stacked at each other, where formulas for magnetic field of solenoids are well known and can be found in any textbook of electromagnetism. If solenoids would be used, they would be positioned exactly at the same places as magnetic dipoles, with their height equal to position of current loops. This would produce magnetic field enclosed right above every solenoid, creating some kind of magnetic membrane with highest magnitude of magnetic field on surface of this membrane and creating very little parasite magnetic field inside of discharge chamber, where actual acceleration of ions takes place. Continuing future research, this is surely the next step of what to change.

Despite the fact that adiabatic approximation is not explicitly defined anywhere in this work, it is a simple definition saying that if adiabatic approximation have to take effect, time change and geometrical change of magnetic field must be lower than *Larmor radius*, which specifies radius of particle drift. As the most significant drift compared to all other drifts is $\mathbf{E} \times \mathbf{B}$ drift, our Larmor radius would be defined as central line of discharge chamber, characterized by equation (3.41). If we look at figure 3.6, we can see that most homogeneous field is in position few millimeters about discharge chamber, which is characterized by $\mathbf{r}_{B_0}$ in equation (3.42). This homogeneity can be seen as place with lowest geometrical change of magnetic field, which can be seen in figure 3.5 as quasi-potential well. This is the exact place where adiabatic approximation would take effect, allowing most stable electron movement, as seen in figure 5.6, 5.9 and 5.10. Place where adiabatic approximation is starting to fail is beautifully seen in figure 5.7 and 5.8, where electron begins to break down and hit the wall of discharge chamber. That is due the fast geometrical change of magnetic field, which can be seen in figure 3.6, 30 millimeters below vector $\mathbf{r}_{B_0}$, exactly at height of all of the magnetic dipoles. For future research, solenoids and their magnetic field, which will create previously described magnetic membrane, would be the best possible candidate for field where adiabatic approximation is valid. This is due to fact that shape of that field would be almost equal to our magnetic field in position $\mathbf{r}_{B_0}$, shown in previously described figure 3.6.

BIBLIOGRAPHY

[1] *Deep Space 1*. NASA. [Online]. Available: http://nmp.jpl.nasa.gov/ds1/.

[2] *SMART-1*. ESA. [Online]. Available: http://www.esa.int/Our˙Activities/Space˙ Science/SMART-1.

[3] Michal Bednařík. *Fyzika 1*. České vysoké učení technické v Praze, Fakulta elektrotechnická, Praha, 2011.

[4] Ira Katz Dan M. Goebel. *Fundamentals of Electric Propulsion: Ion and Hall Thrusters*. John Wiley & Sons, 22-12-2008. ISBN 9780470436264. [Online]. Available: http://descanso.jpl.nasa.gov/SciTechBook/series1/Goebel¨cmprsd˙opt.pdf.

[5] Aleš Holub. Sonda deep space 1. In *MEK - Malá encyklopedie kosmonautiky*. 28-4-2002. [Online]. Available: http://mek.kosmo.cz/sondy/usa/ds1/index.htm.

[6] Frank Stanley Gulczinski III. *Examination of the structure and evolution of ion energy properties of a 5 kW class laboratory hall effect thruster at various operational conditions*. PhD thesis, The University of Michigan, 1999. [Online]. Available: http://www.pepl.engin.umich.edu/pdf/1999˙gulczinski˙thesis.pdf.

[7] M. J. Patterson J. S. Sovey, V. K. Rawlin. Ion propulsion development projects in u. s.: Space electric rocket test 1 to deep space 1. In *Journal of Propulsion and Power, Vol. 17, No. 3*. Pisa, Italy, 2001. [Online]. Available: http://www.spaceatdia.org/ uploads/mariano/ep2/Magnetoplasmadynamic%20Thrusters.pdf.

[8] Petr Kulhánek. *Úvod do teorie plazmatu*. AGA, Praha, 2011. ISBN 978-80-904582-2-2.

[9] Jozef Kvasnica. *Teorie elektromagnetického pole*. ACADEMIA Praha, Praha, 1985.